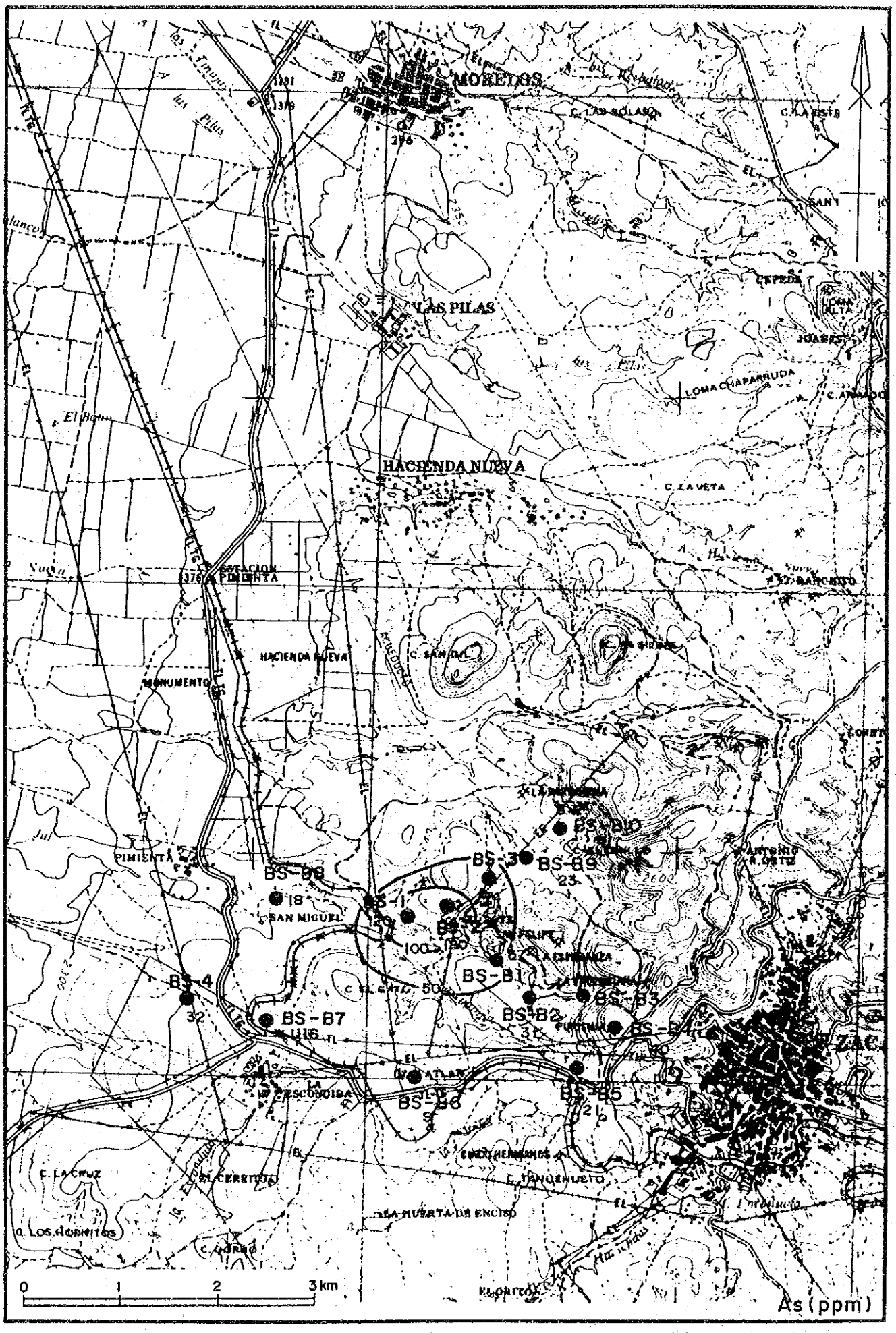

Fig. 3-5-1 Analysis Map of Chemical Data of Soil (8)

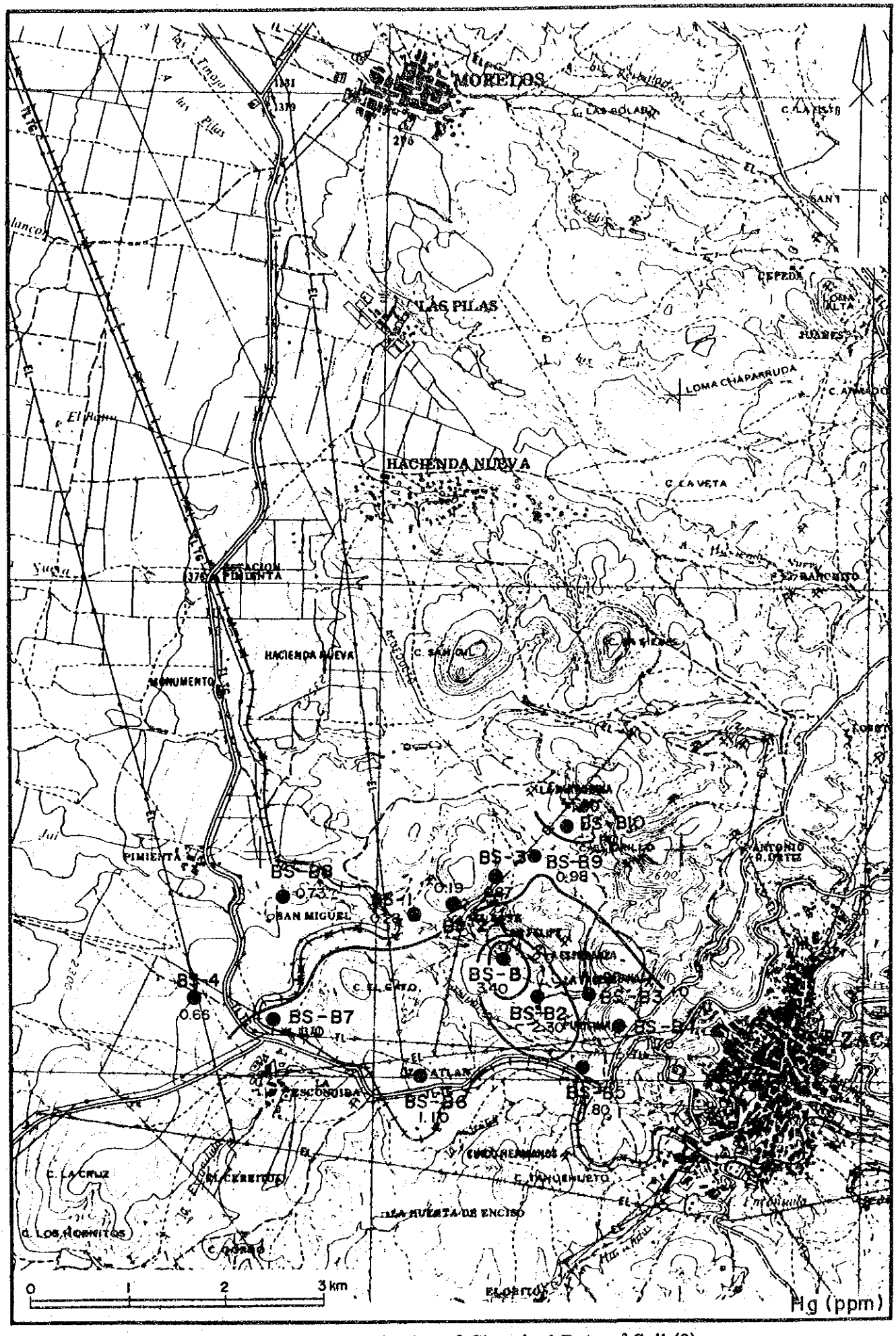

Fig. 3-5-1 Analysis Map of Chemical Data of Soil (9)

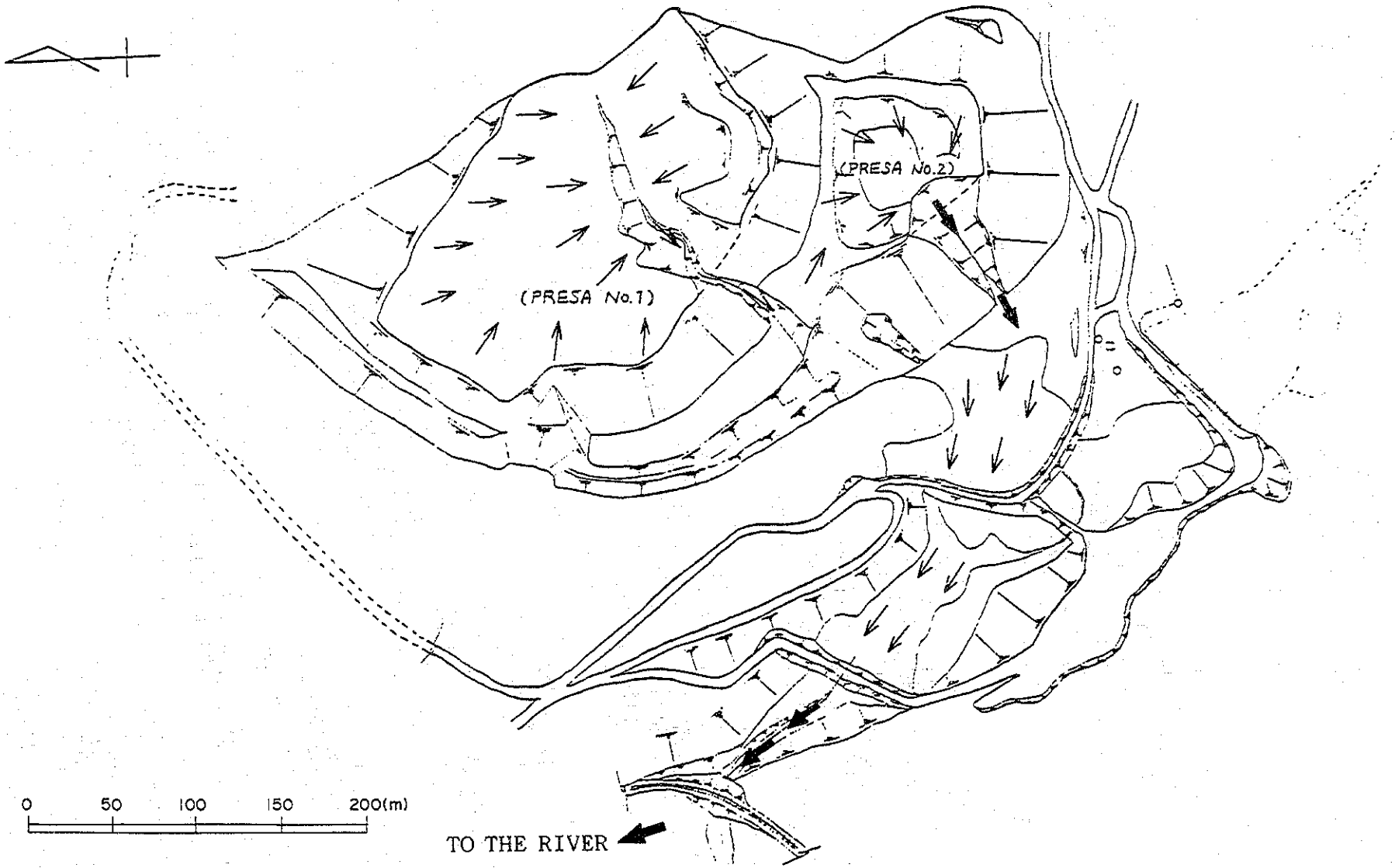

Fig. 3-6-1 The Flow of Rainwater

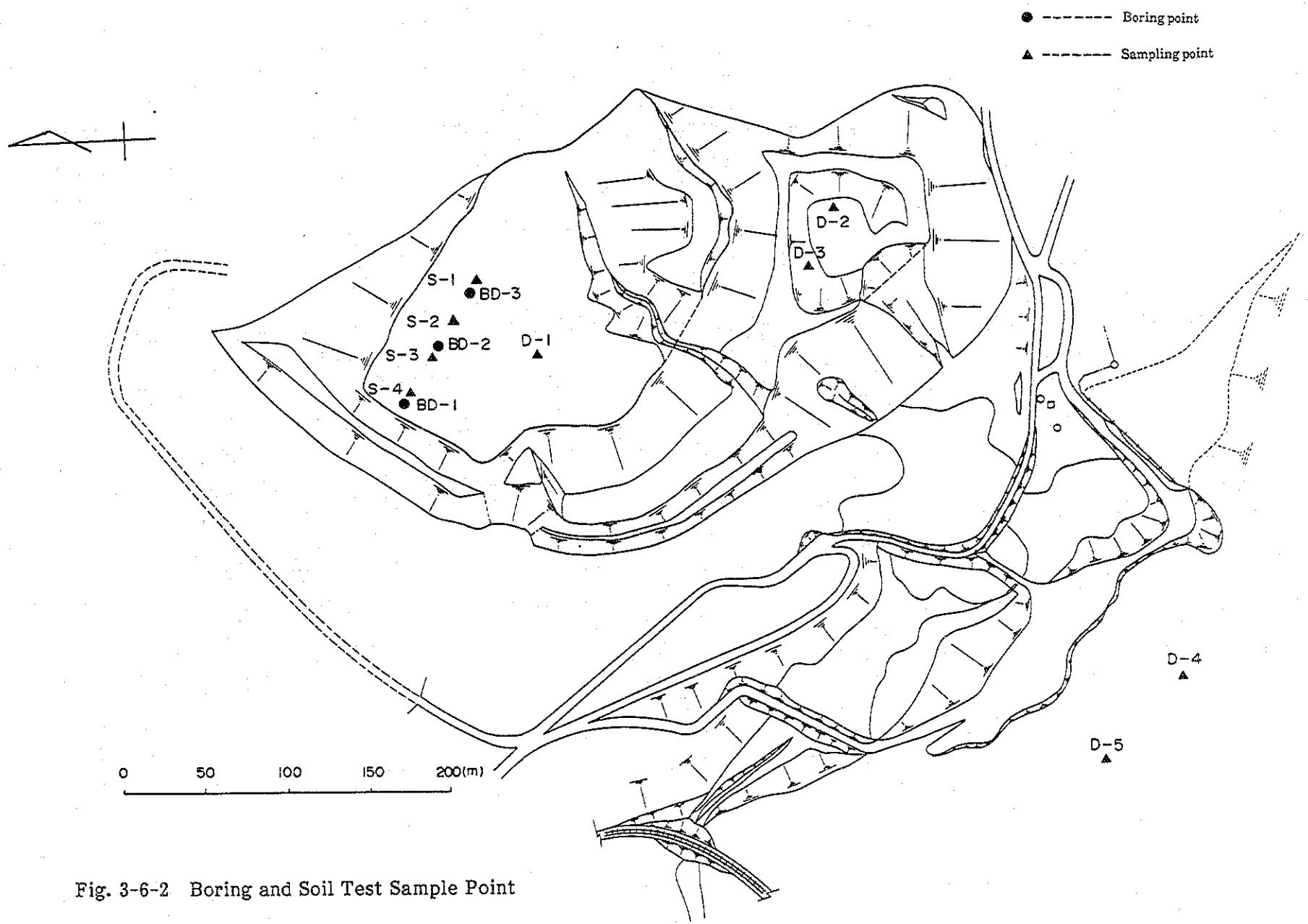

Fig. 3-6-2 Boring and Soil Test Sample Point

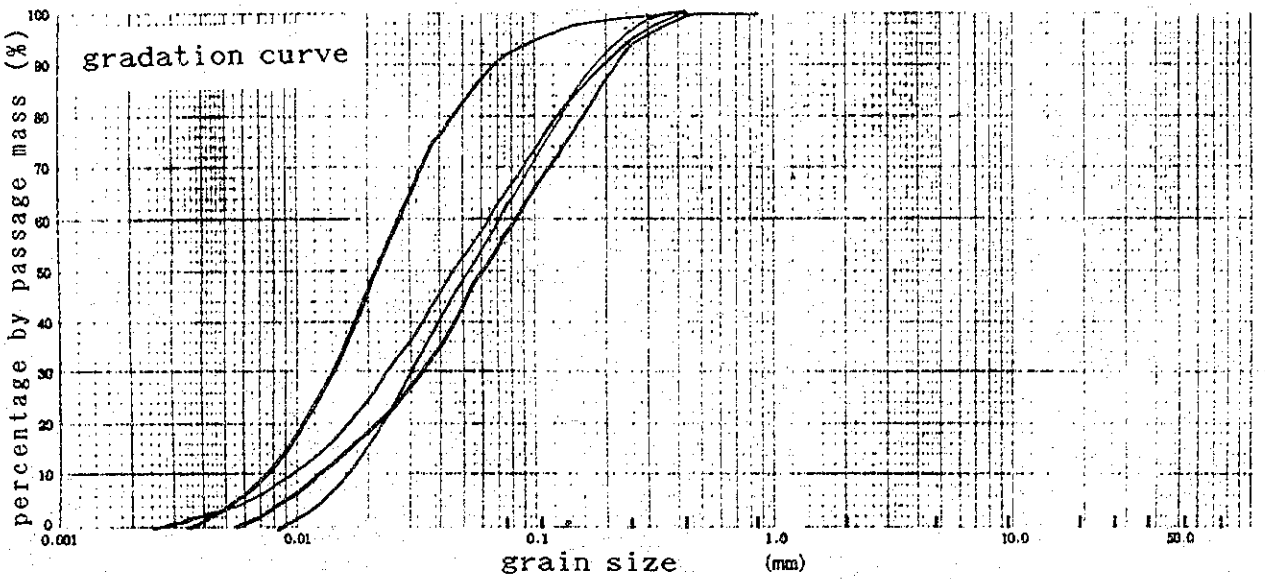

Fig. 3-6-3 Grain Size Accumulation Curve

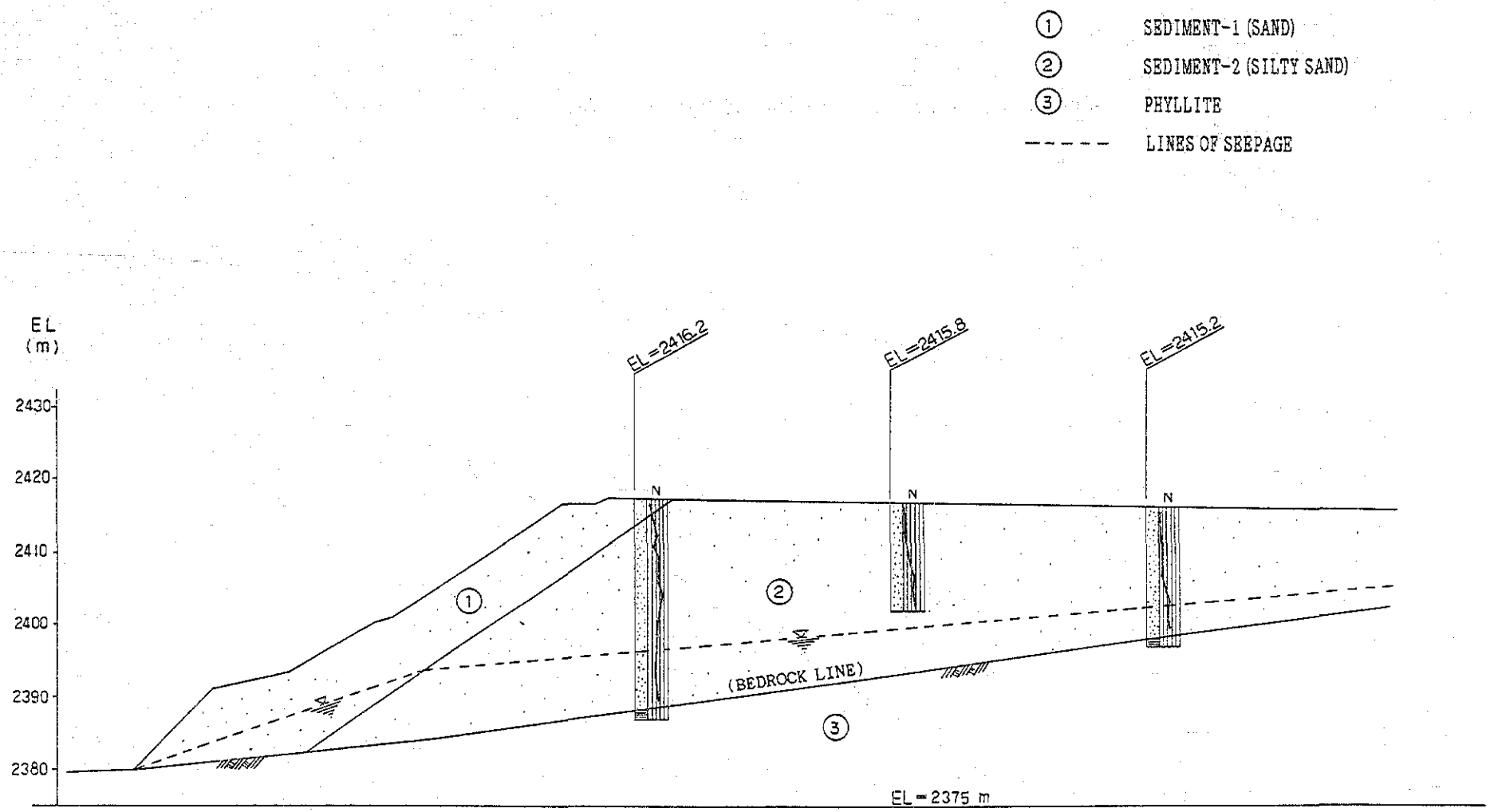

Fig. 3-6-4 El Bote Tailing Dam Geological Cross Section

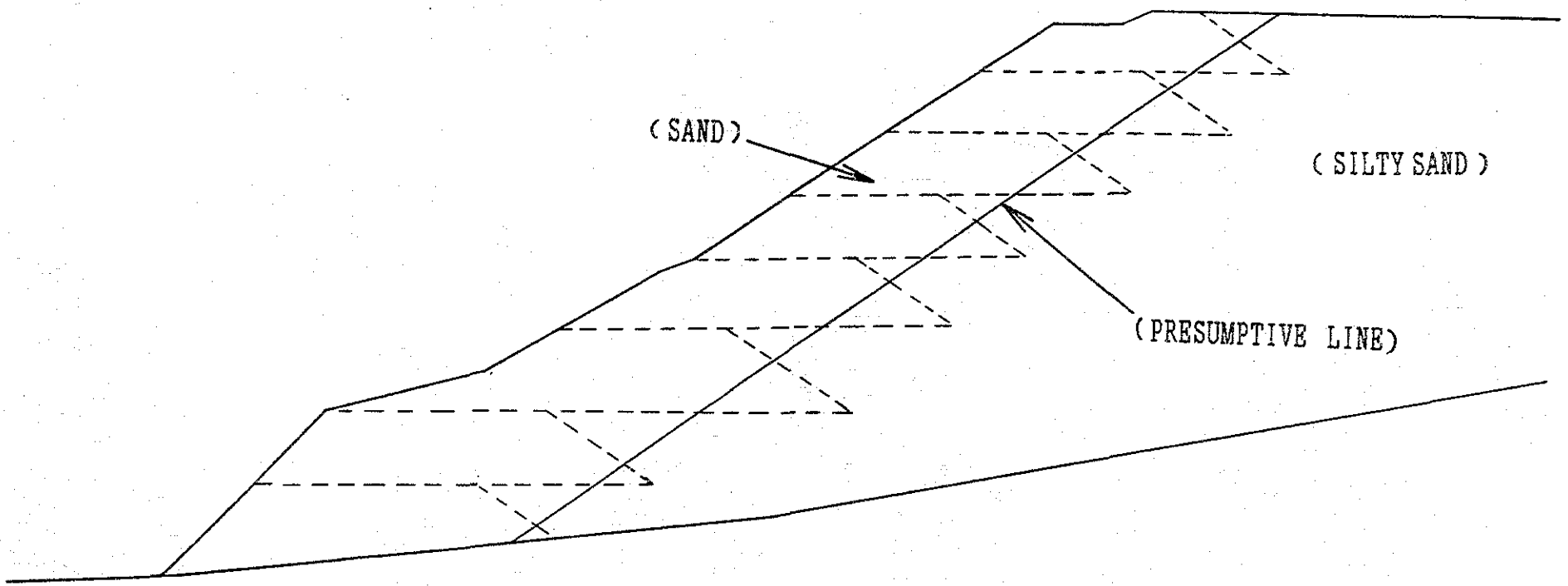

Fig. 3-6-5 The Method for Presumption of Border Line

CONDITION OF SOIL

Zone No.	SOIL	PARTIAL SATURATION DENSITY ρ_t (g/cm³)	SATURATION DENSITY ρ_{sat} (g/cm³)	COHESION C (kgf/cm²)	SHEARING RESISTANCE ANGLE ϕ (°)
①	SEDIMENT－1	1.736	1.933	0.00	30.0
②	SEDIMENT－2	1.774	1.810	0.10	23.0

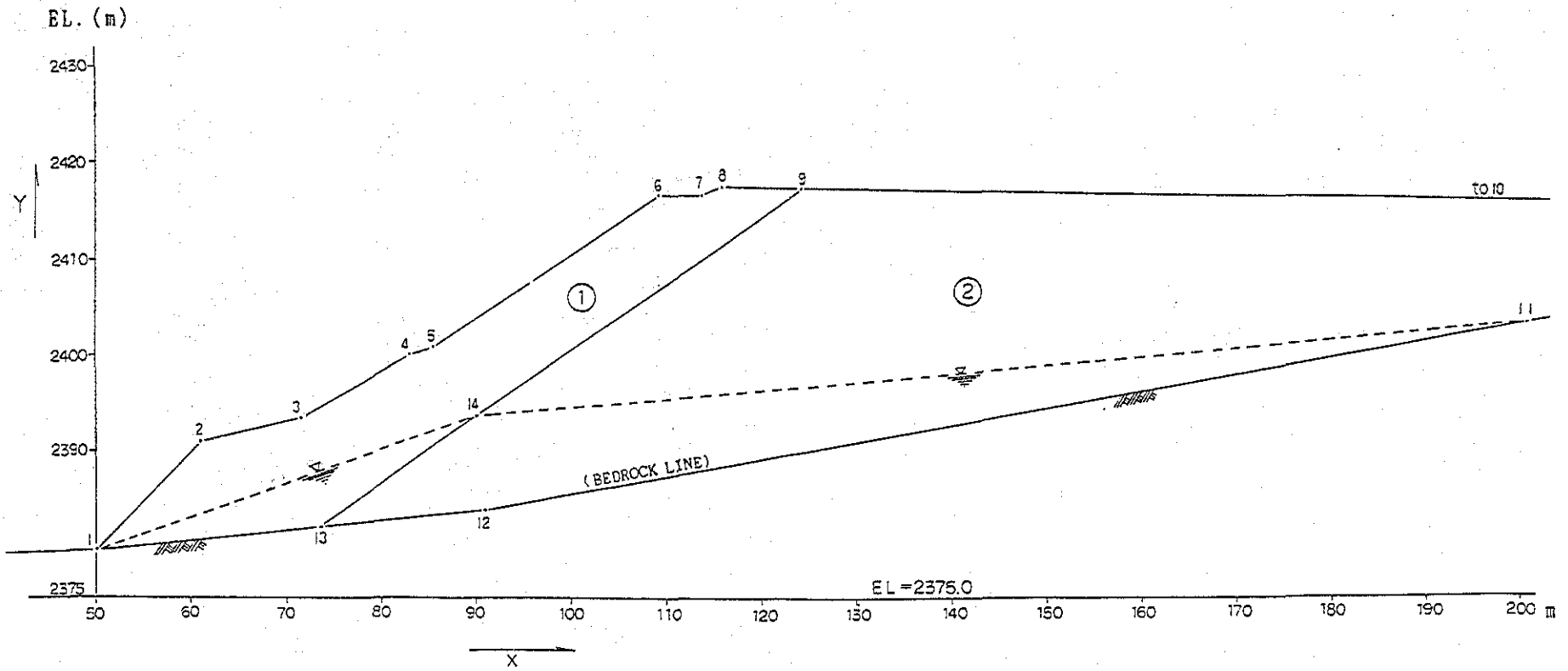

Fig. 3-6-6 The Model of Tailing Dam Stability Analysis

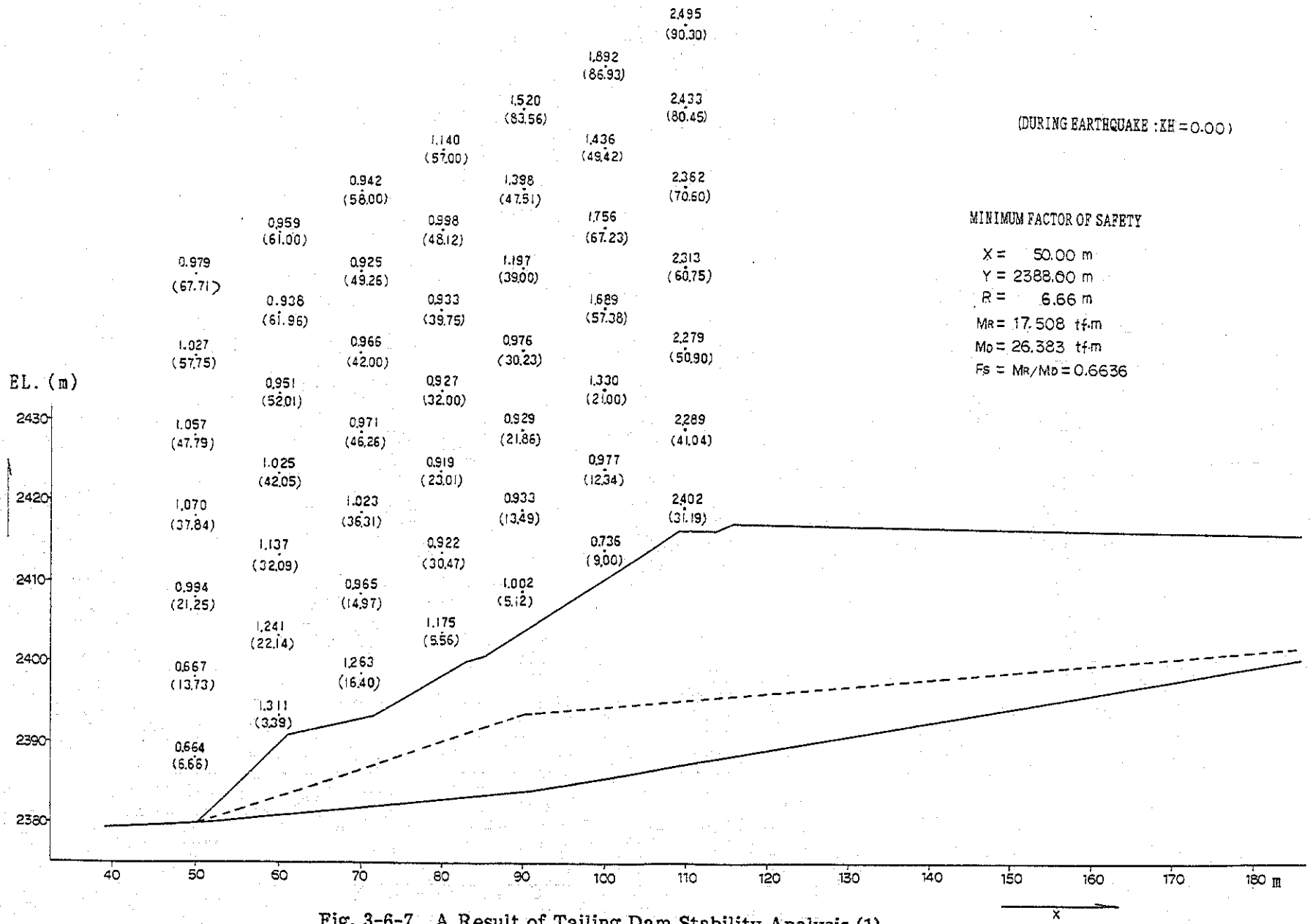

Fig. 3-6-7 A Result of Tailing Dam Stability Analysis (1)

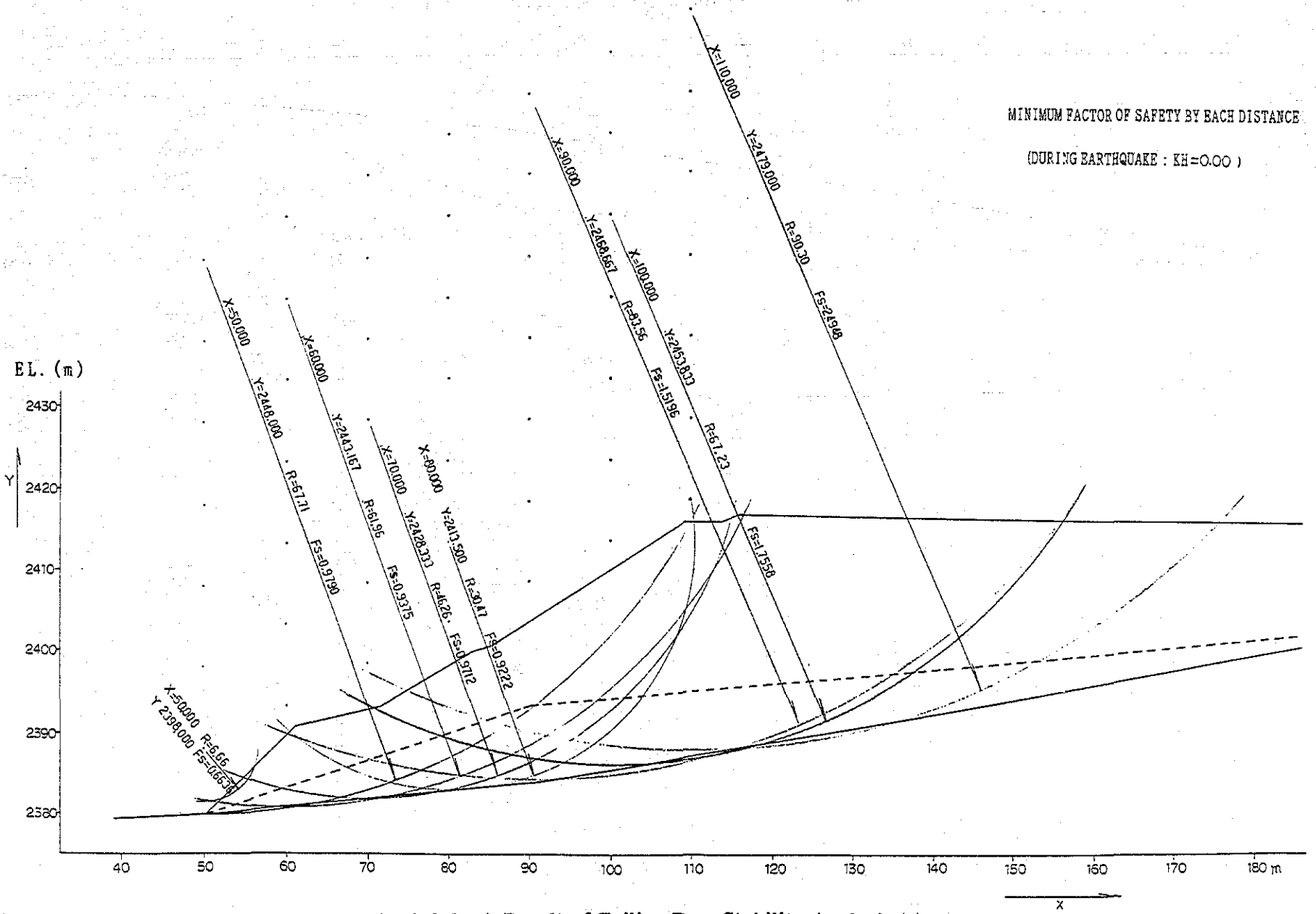

Fig. 3-6-8 A Result of Tailing Dam Stability Analysis (2)

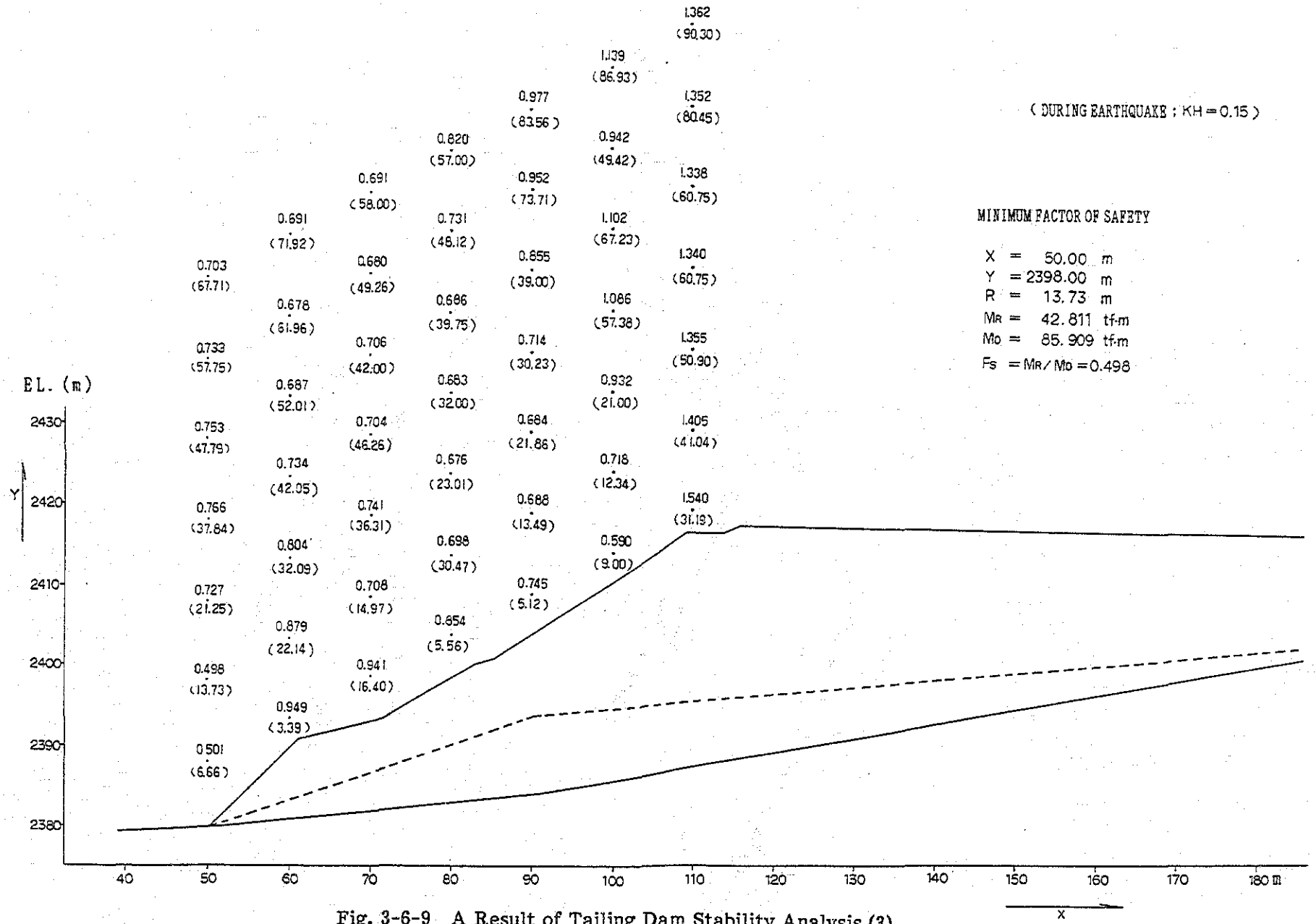

Fig. 3-6-9 A Result of Tailing Dam Stability Analysis (3)

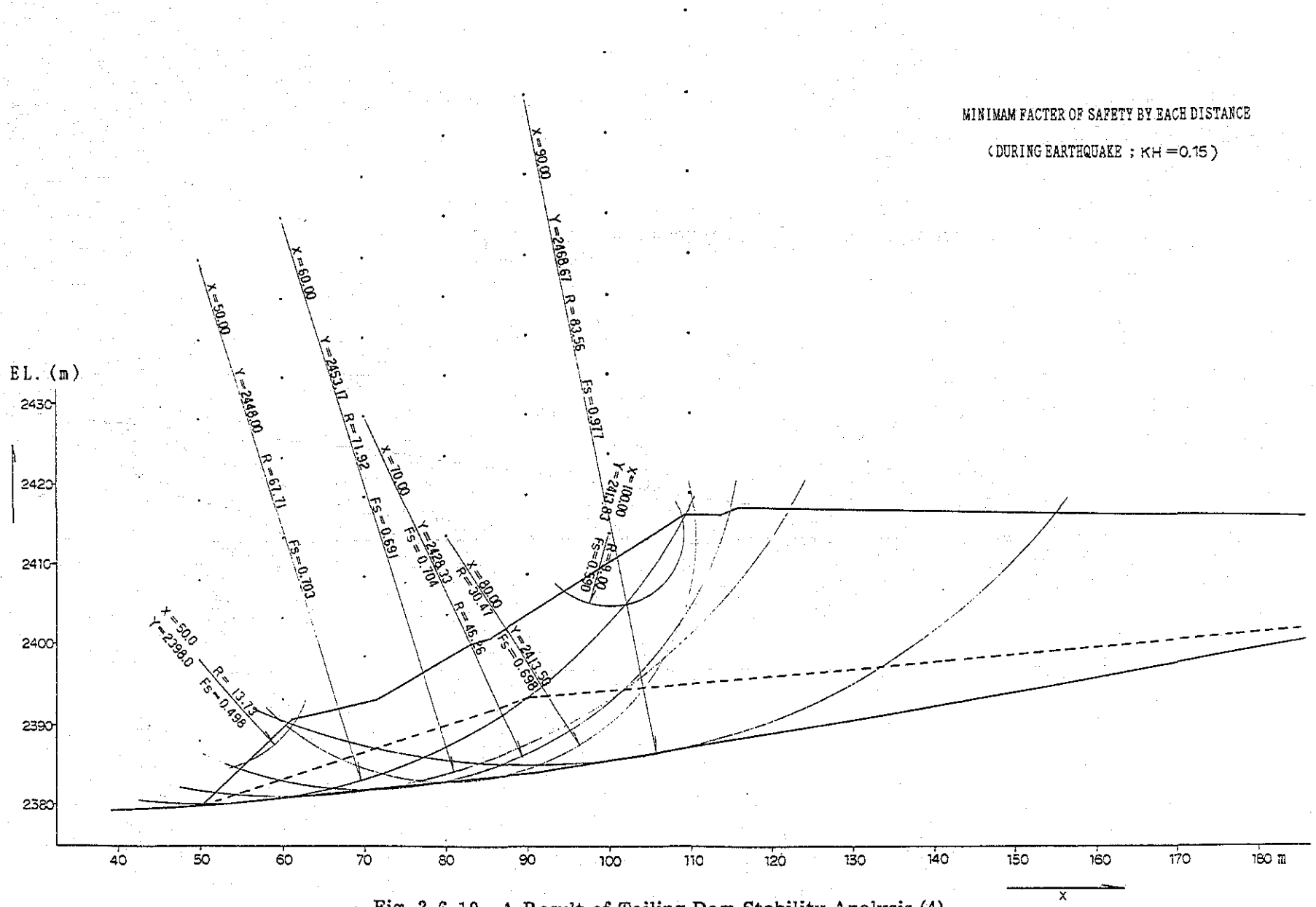

Fig. 3-6-10 A Result of Tailing Dam Stability Analysis (4)

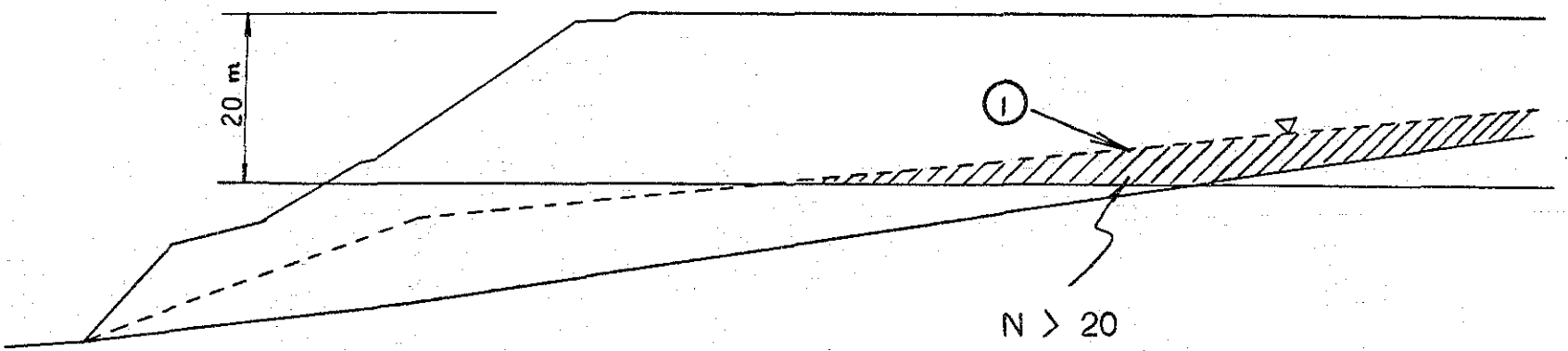

Fig. 3-6-11 The Scope for Danger of Liquefaction

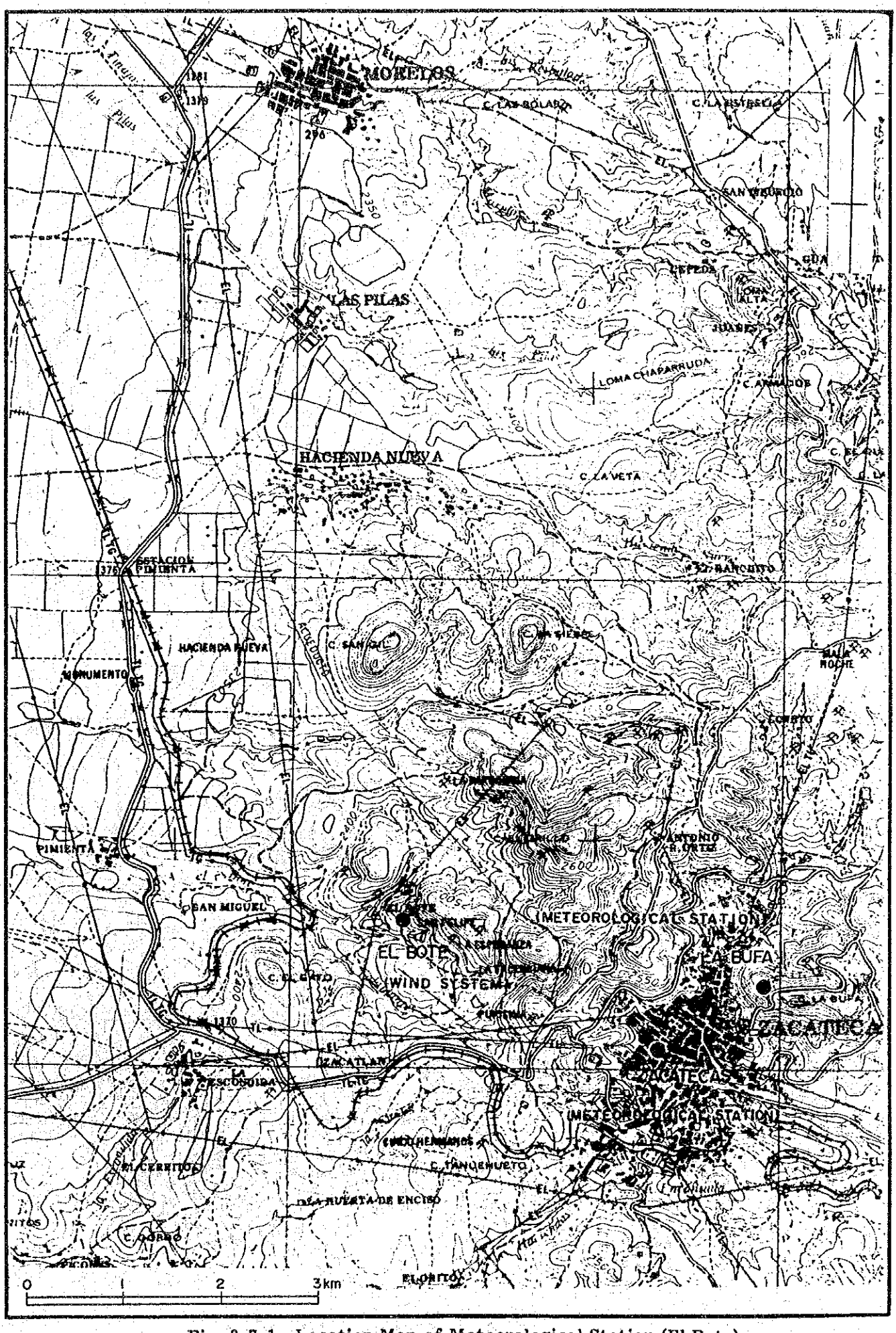

Fig. 3-7-1 Location Map of Meteorological Station (El Bote)

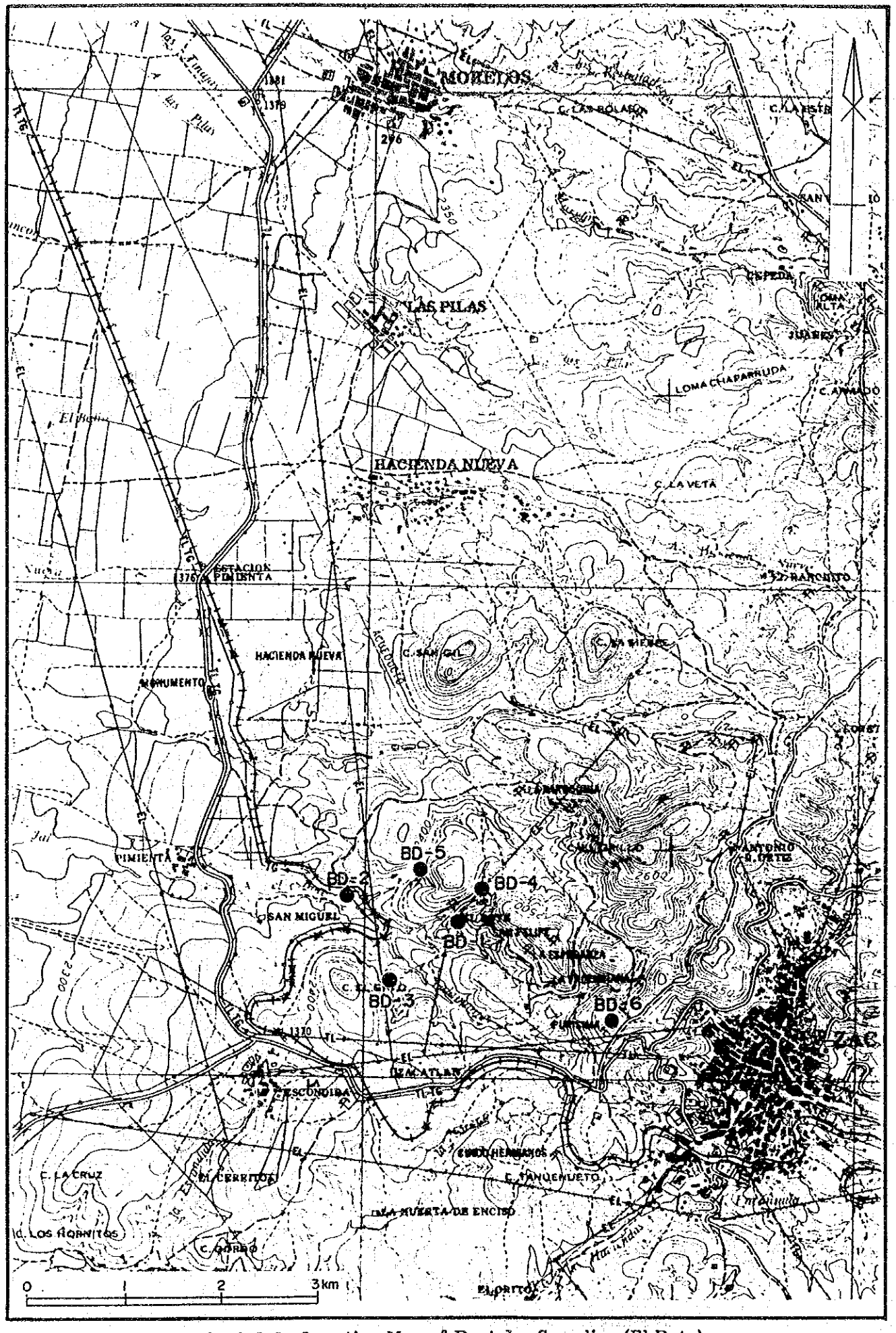

Fig. 3-7-2 Location Map of Dust Jar Sampling (El Bote)

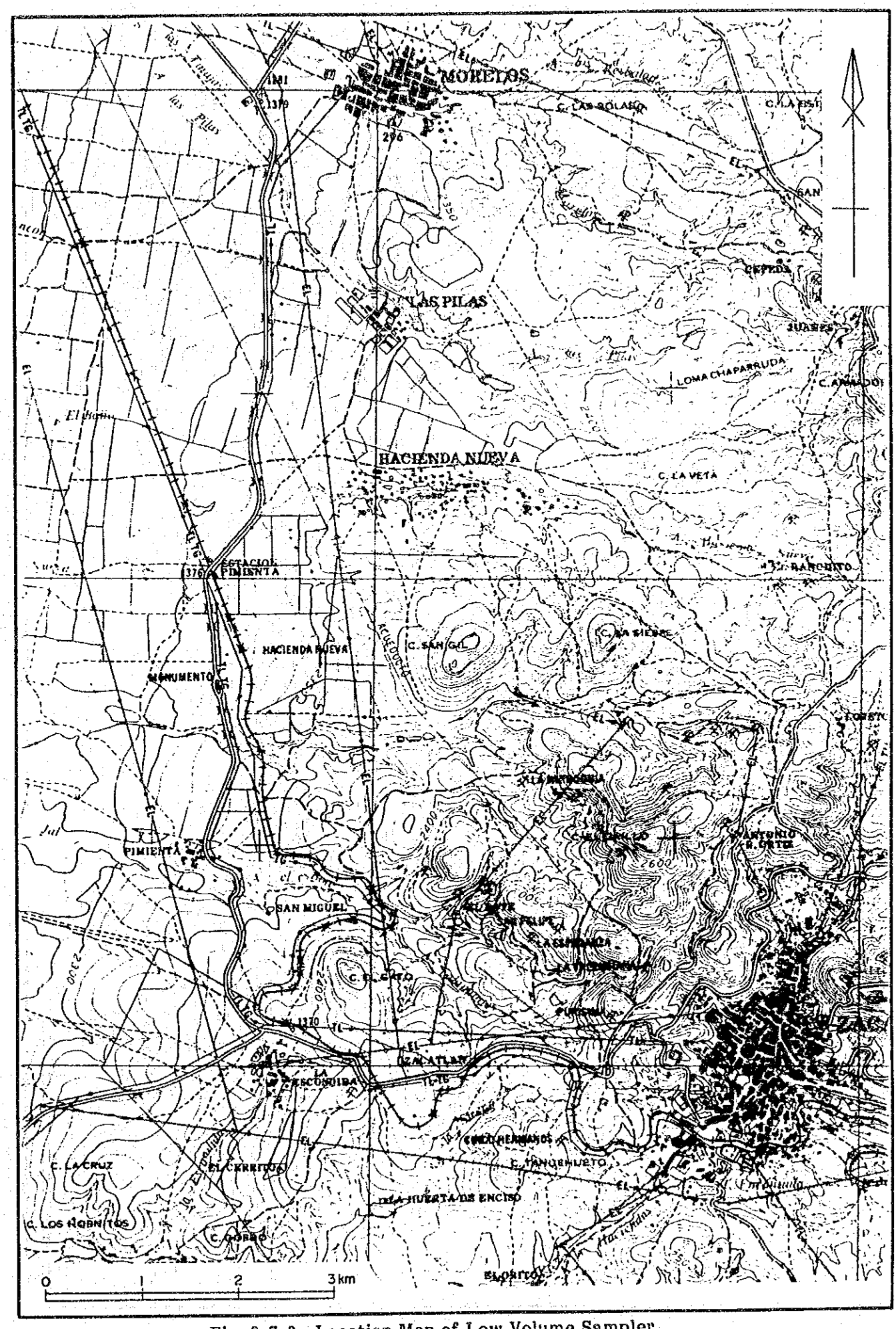

Fig. 3-7-3 Location Map of Low Volume Sampler

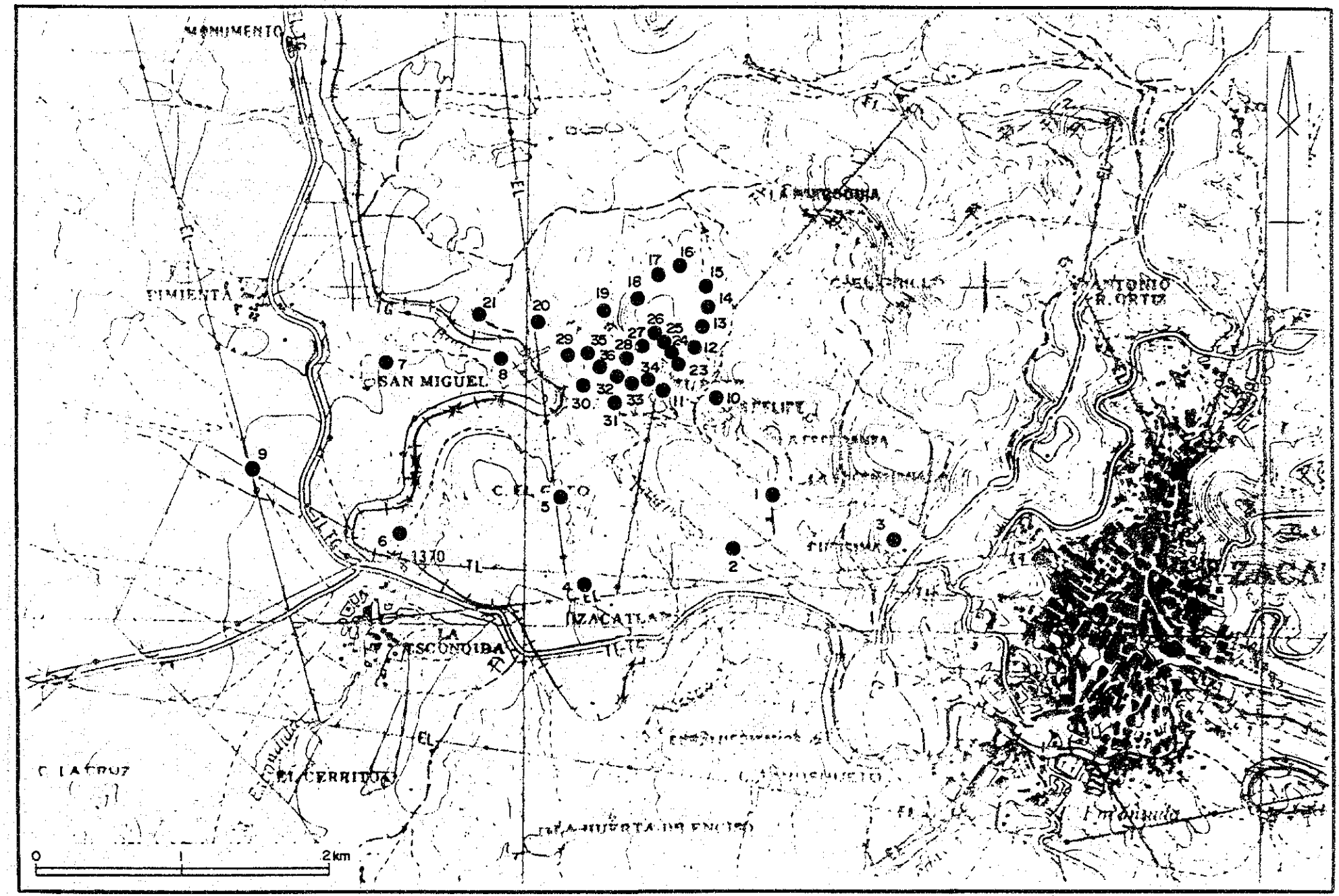

Fig. 3-7-4 Location Map of Digital Dust Monitors (El Bote)

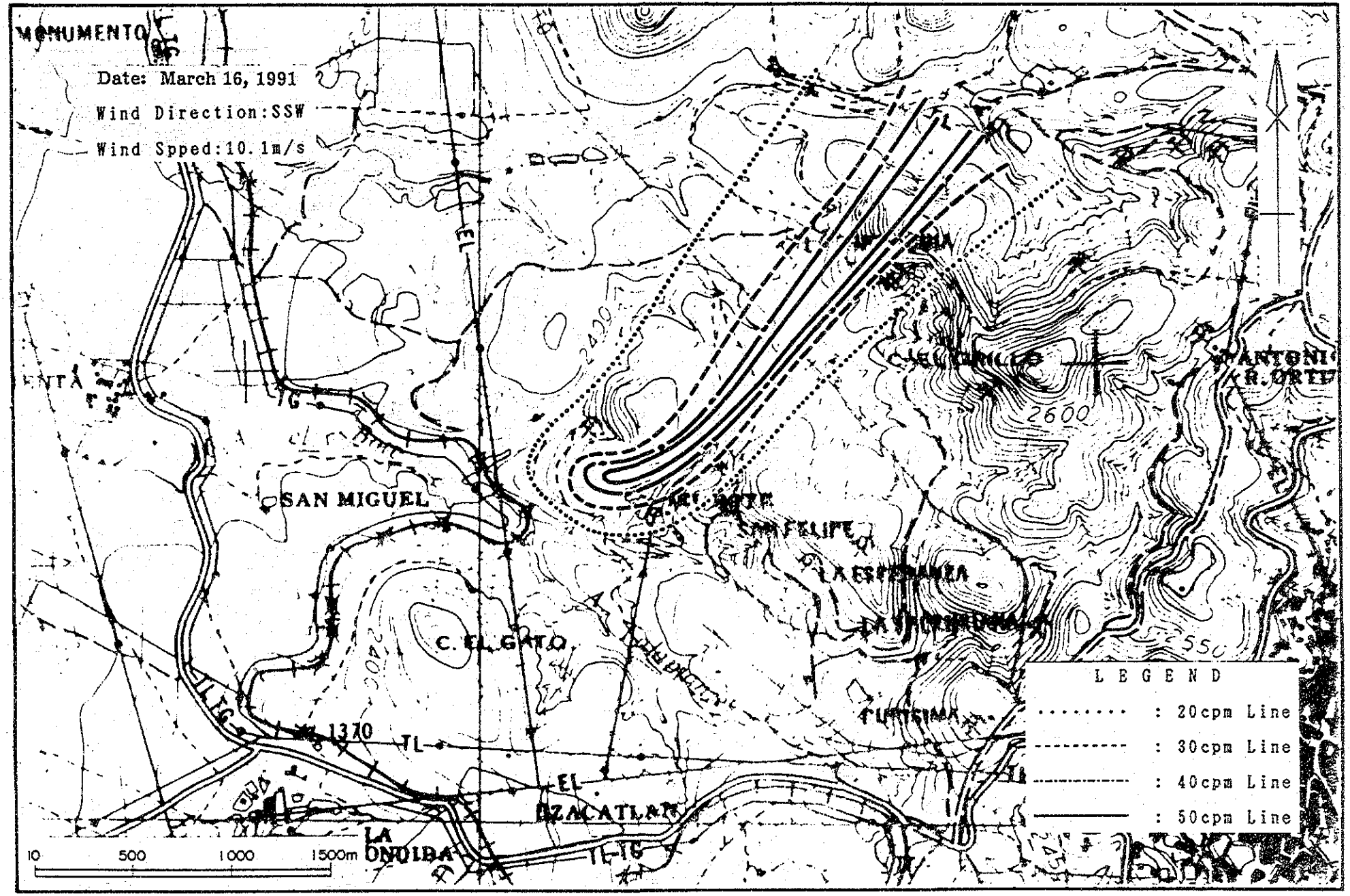

Fig. 3-7-5 Analysis Map of Digital Dust Monitors (El Bote) (1)

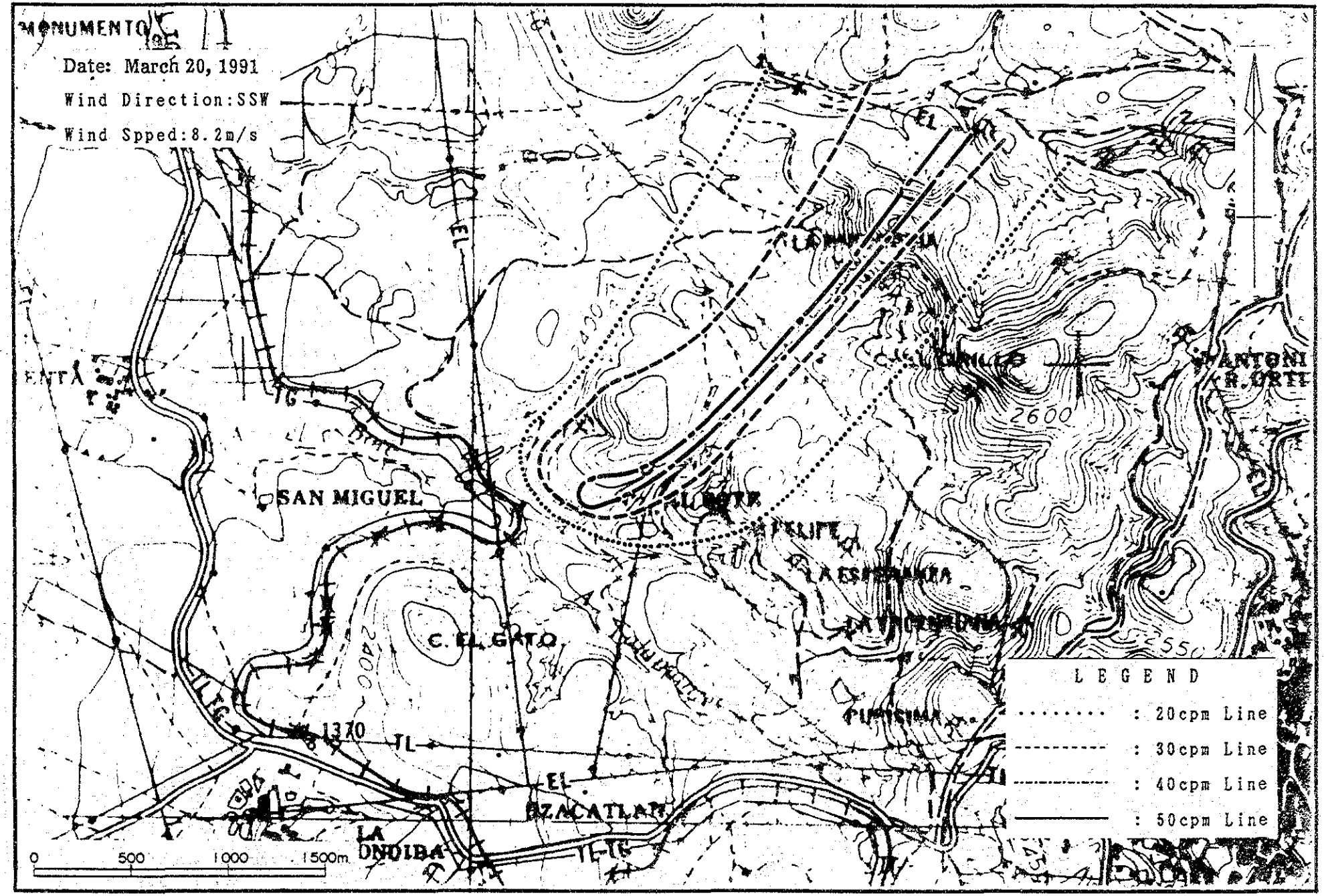

Fig. 3-7-5 Analysis Map of Digital Dust Monitors (El Bote) (2)

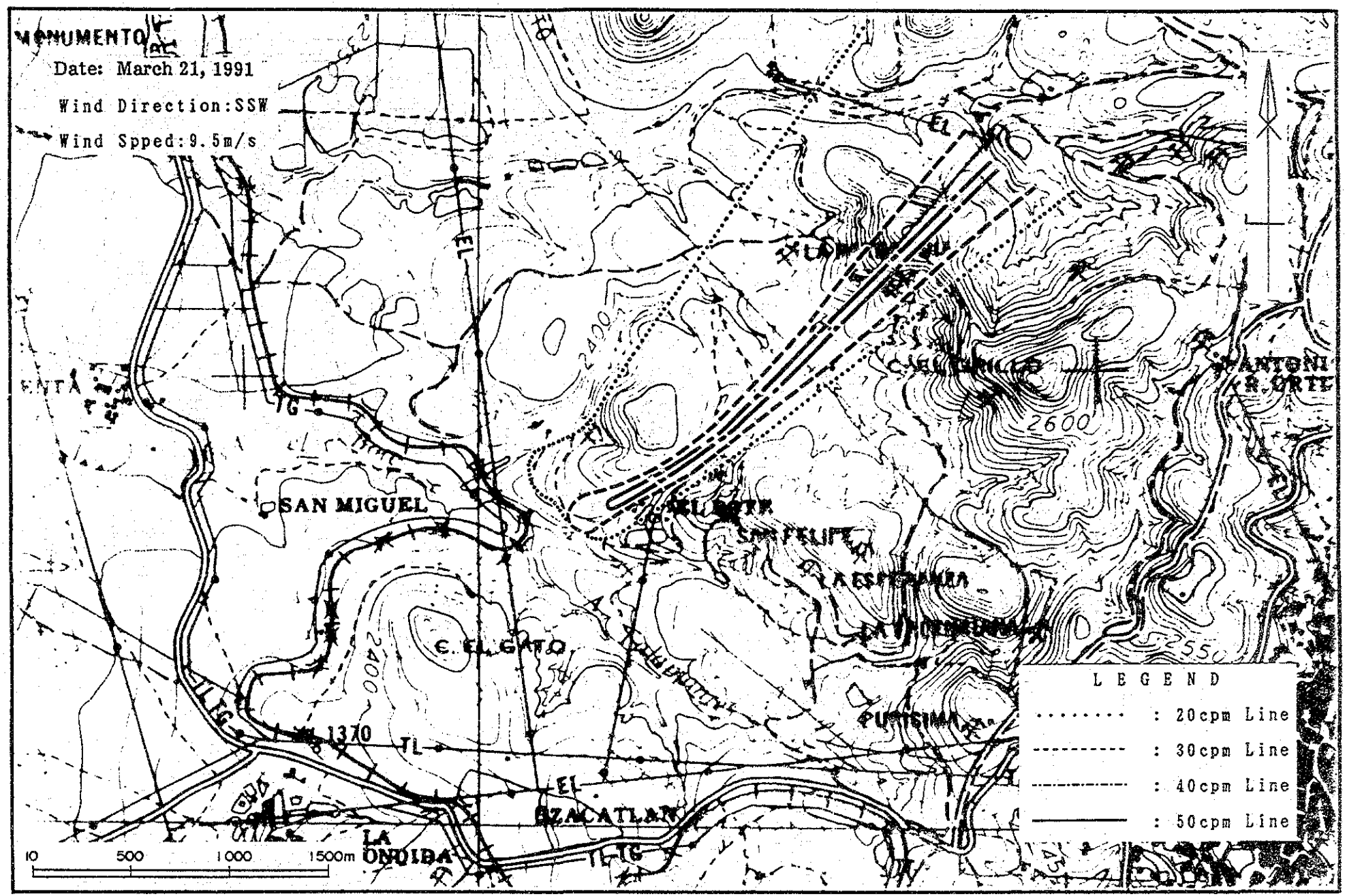

Fig. 3-7-5 Analysis Map of Digital Dust Monitors (El Bote) (3)

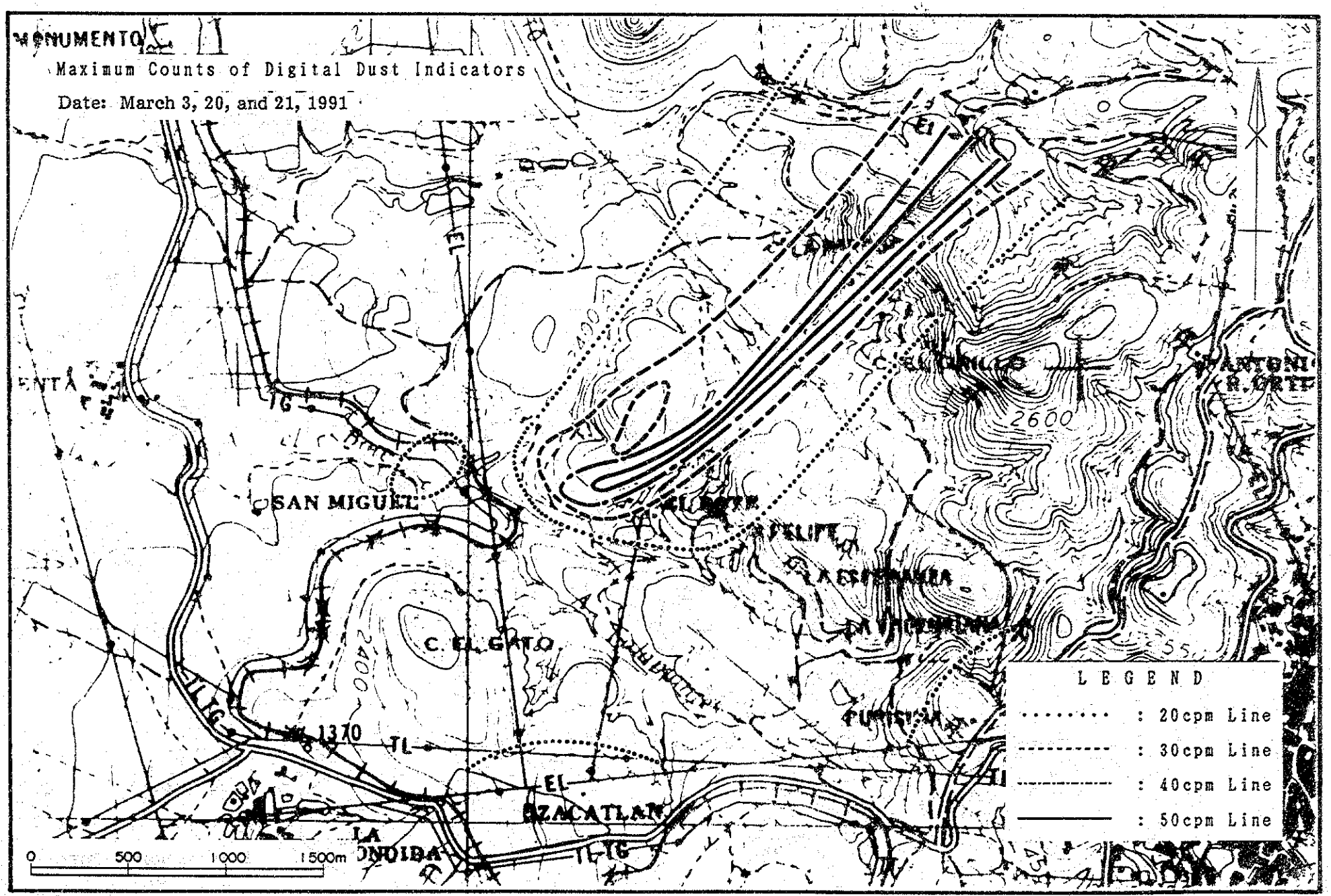

Fig. 3-7-5 Analysis Map of Digital Dust Monitors (El Bote) (4)

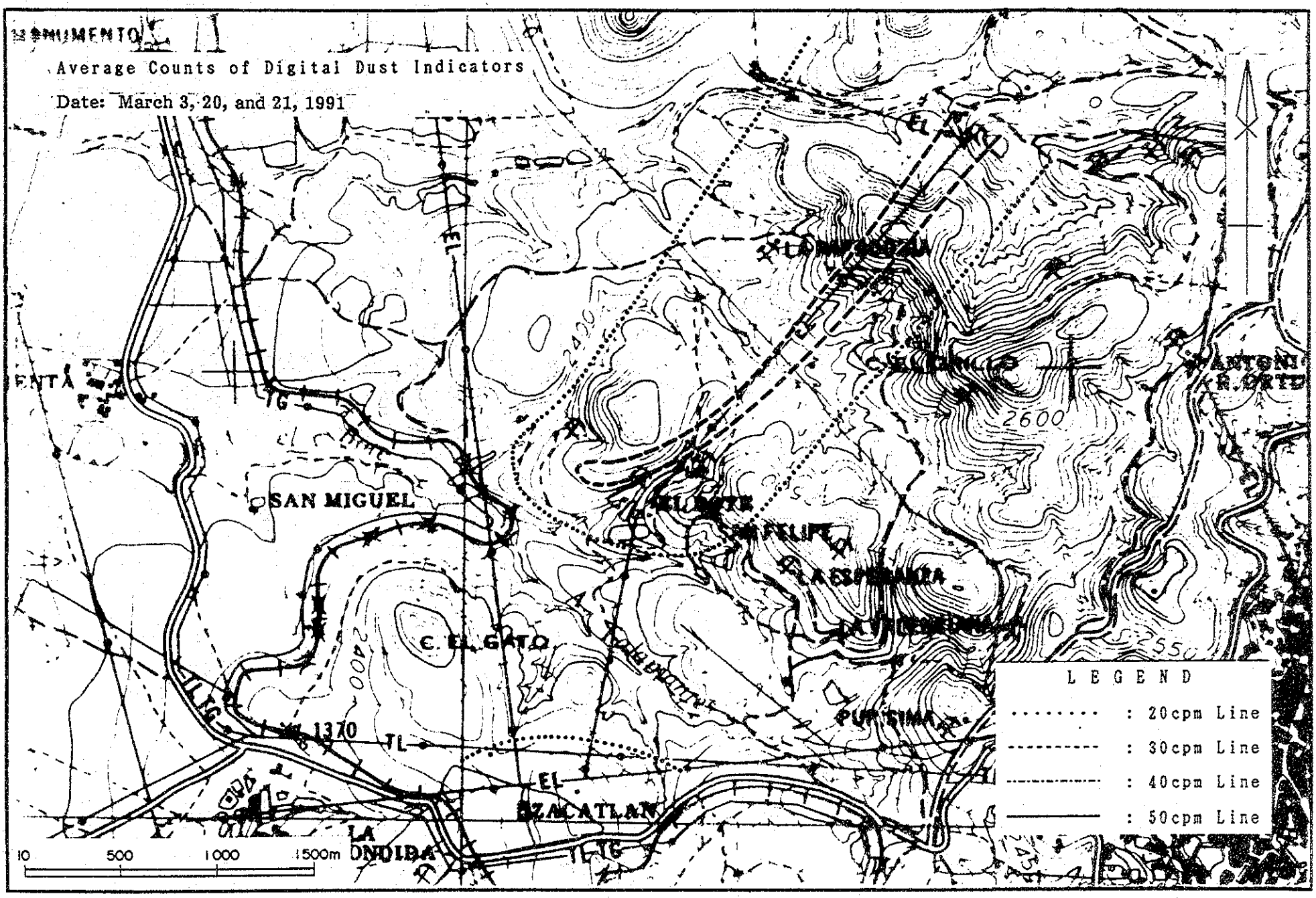

Fig. 3-7-5 Analysis Map of Digital Dust Monitors (El Bote) (5)

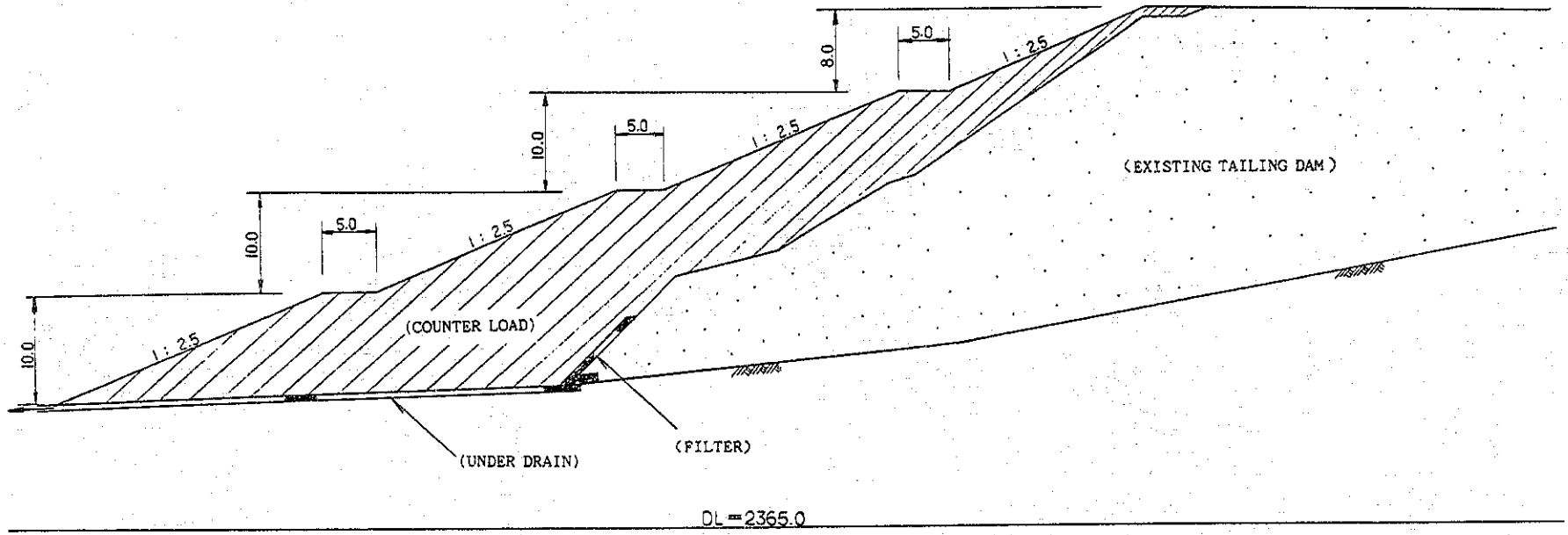

Fig. 3-9-1 The Model of Counter Load

EL BOTE TAILING DAM

CONDITION OF SOIL

Zone No.	SOIL	PARTIAL SATURATION DENSITY ρ_t (g/cm³)	SATURATION DENSITY ρ_{sat} (g/cm³)	COHESION C (kgf/cm²)	SHEARING RESISTANCE ANGLE ϕ (°)
①	GRAVEL	1.800	1.912	0.00	37.0
②	SEDIMENT-1	1.736	1.933	0.00	30.0
③	SEDIMENT-2	1.774	1.810	0.10	23.0

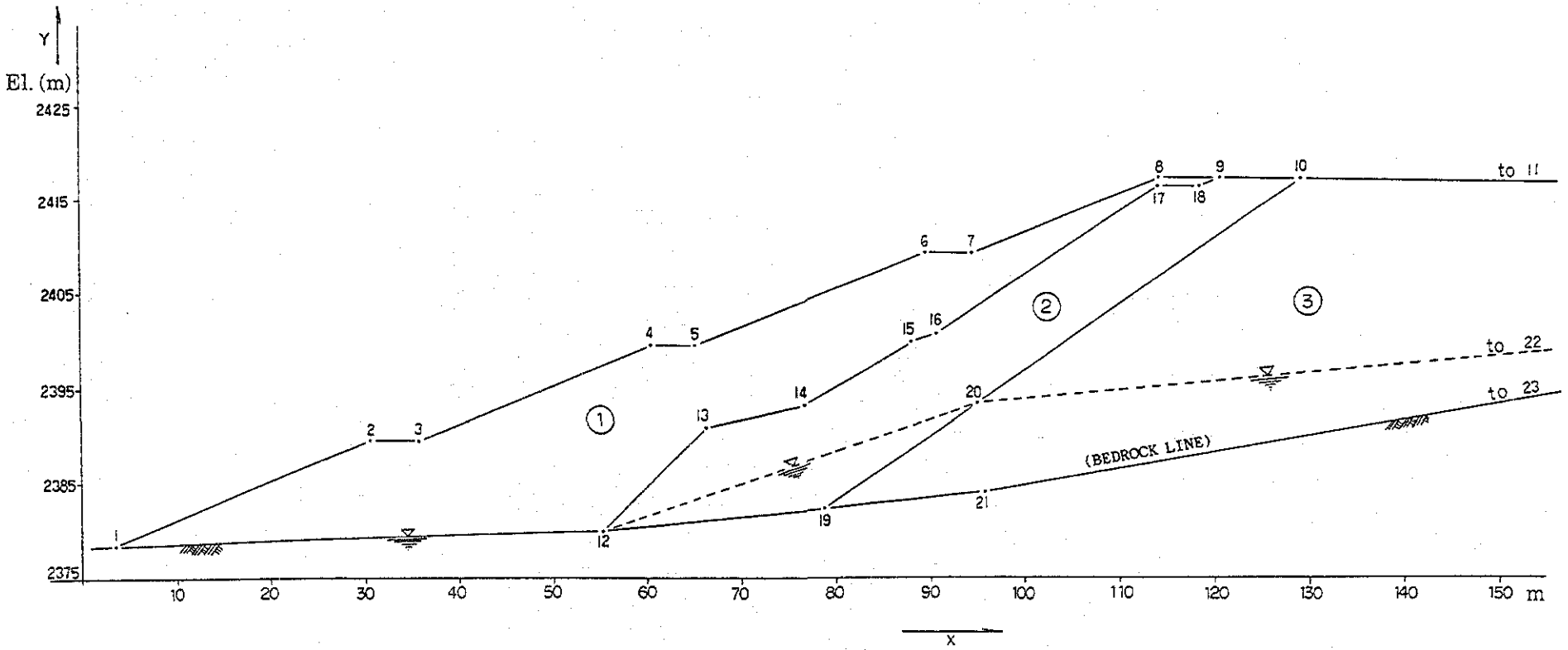

Fig. 3-9-2 The Model of Tailing Dam Stability Analysis

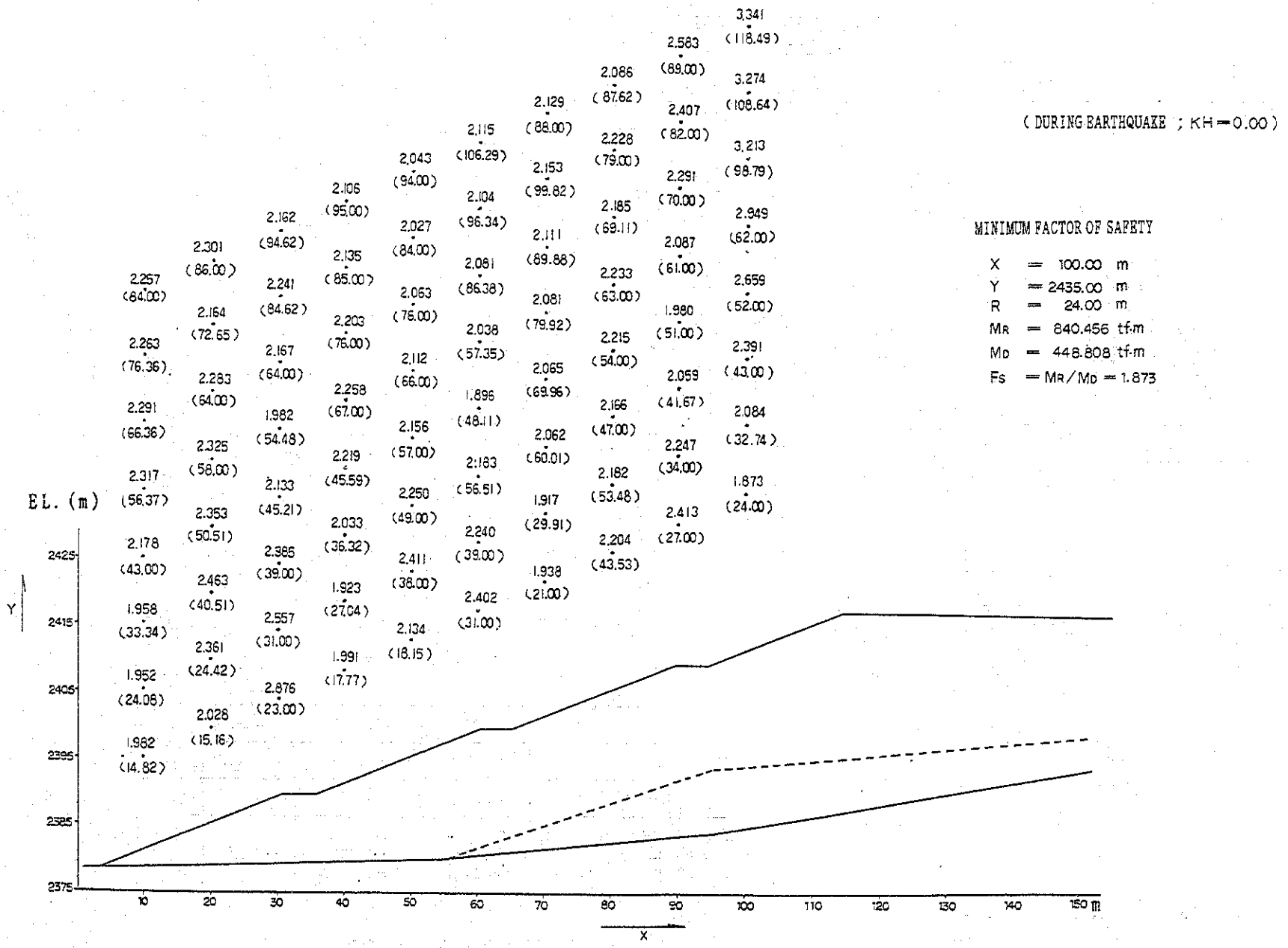

Fig. 3-9-3 A Result of Tailing Dam Stability Analysis (1)

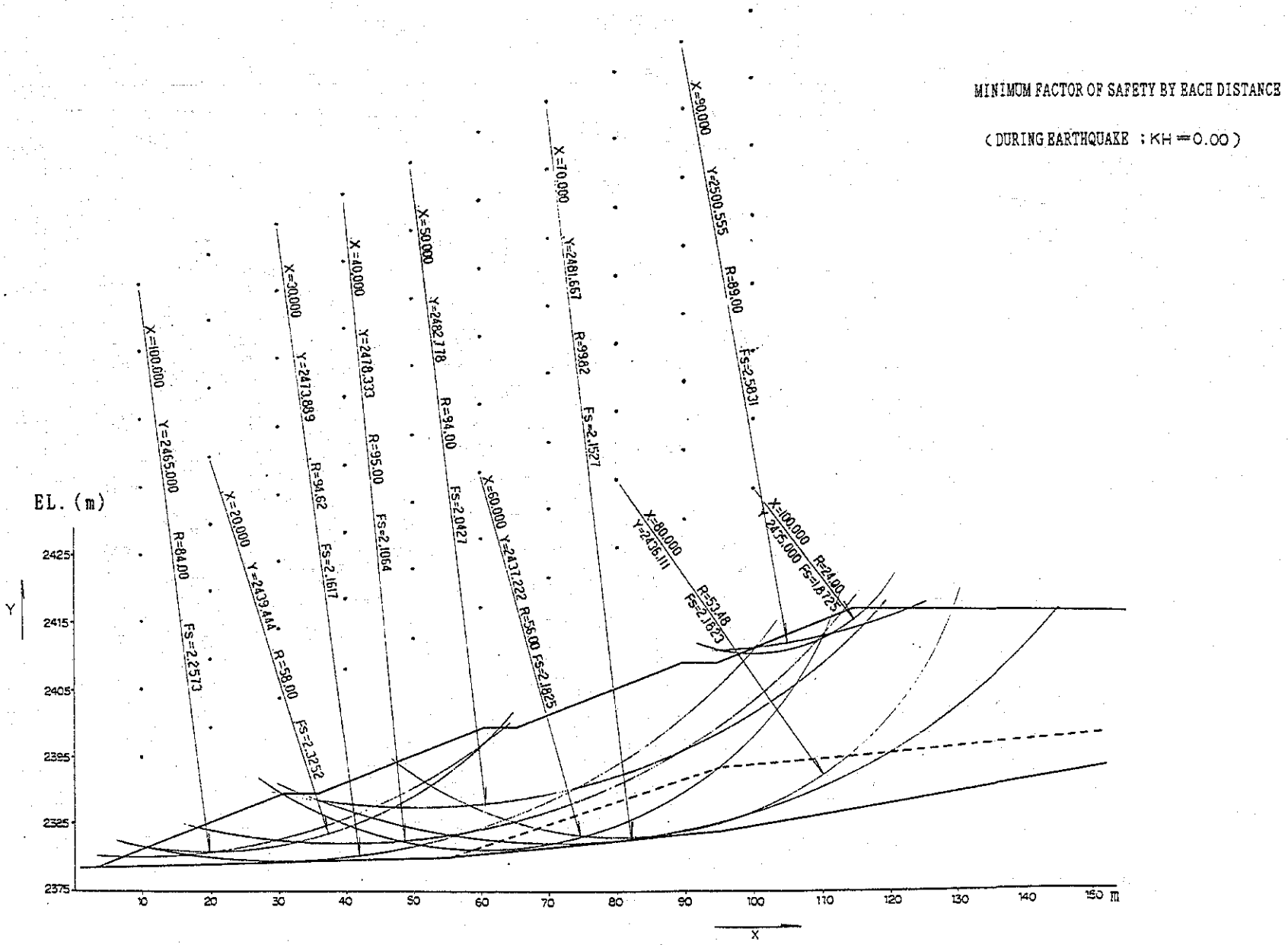

Fig. 3-9-4 A Result of Tailing Dam Stability Analysis (2)

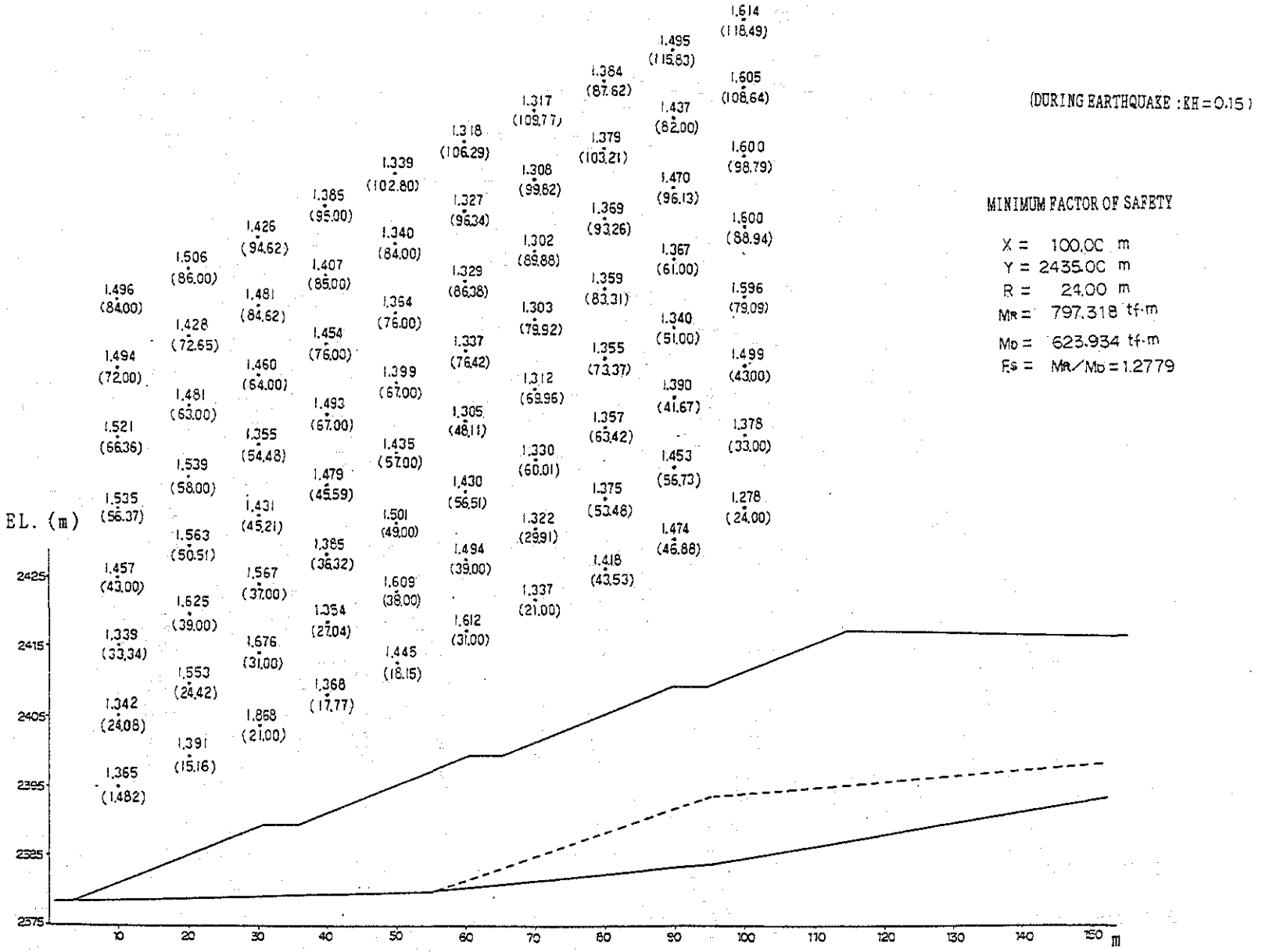

Fig. 3-9-5 A Result of Tailing Dam Stability Analysis (3)

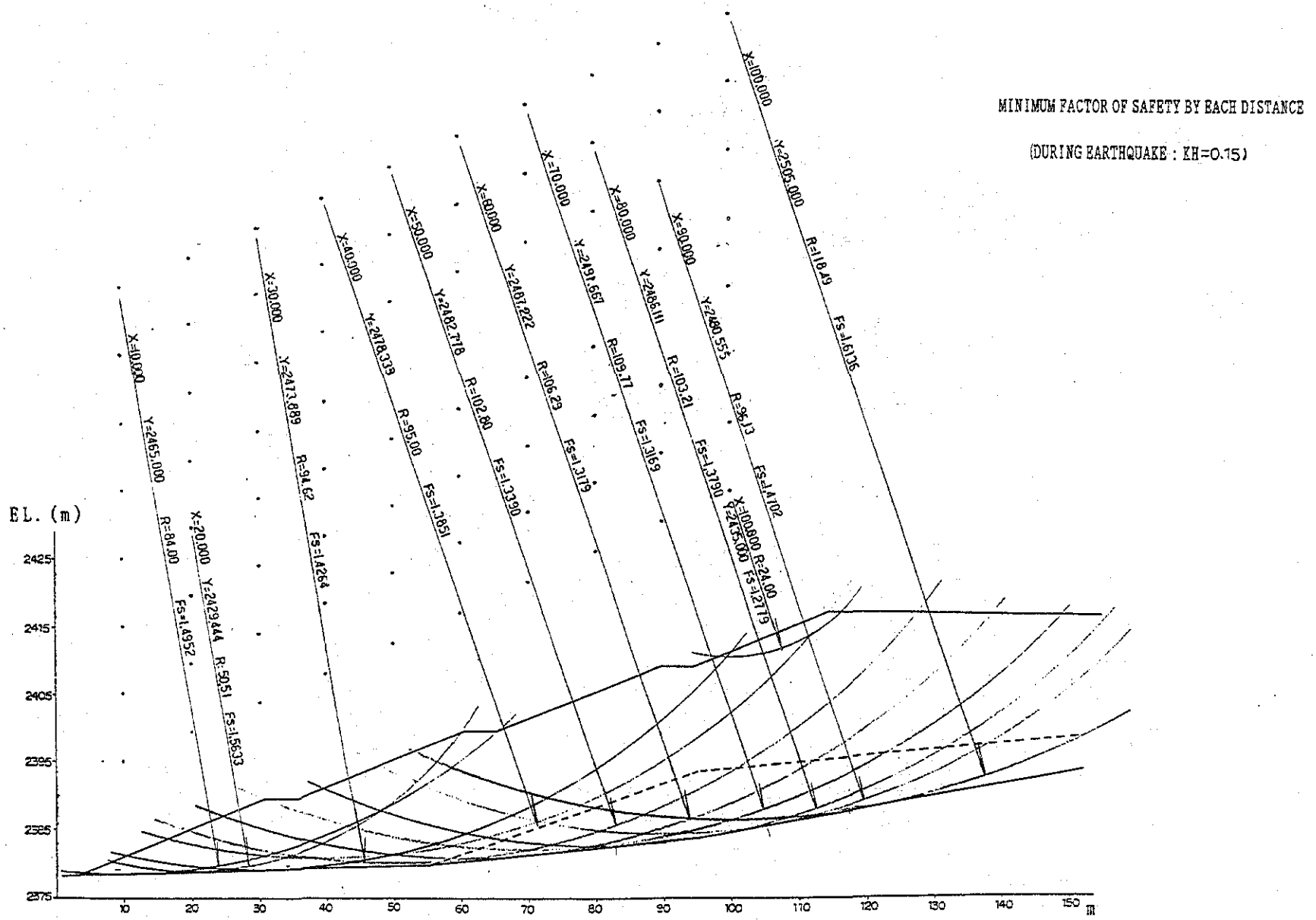

Fig. 3-9-6 A Result of Tailing Dam Stability Analysis (4)

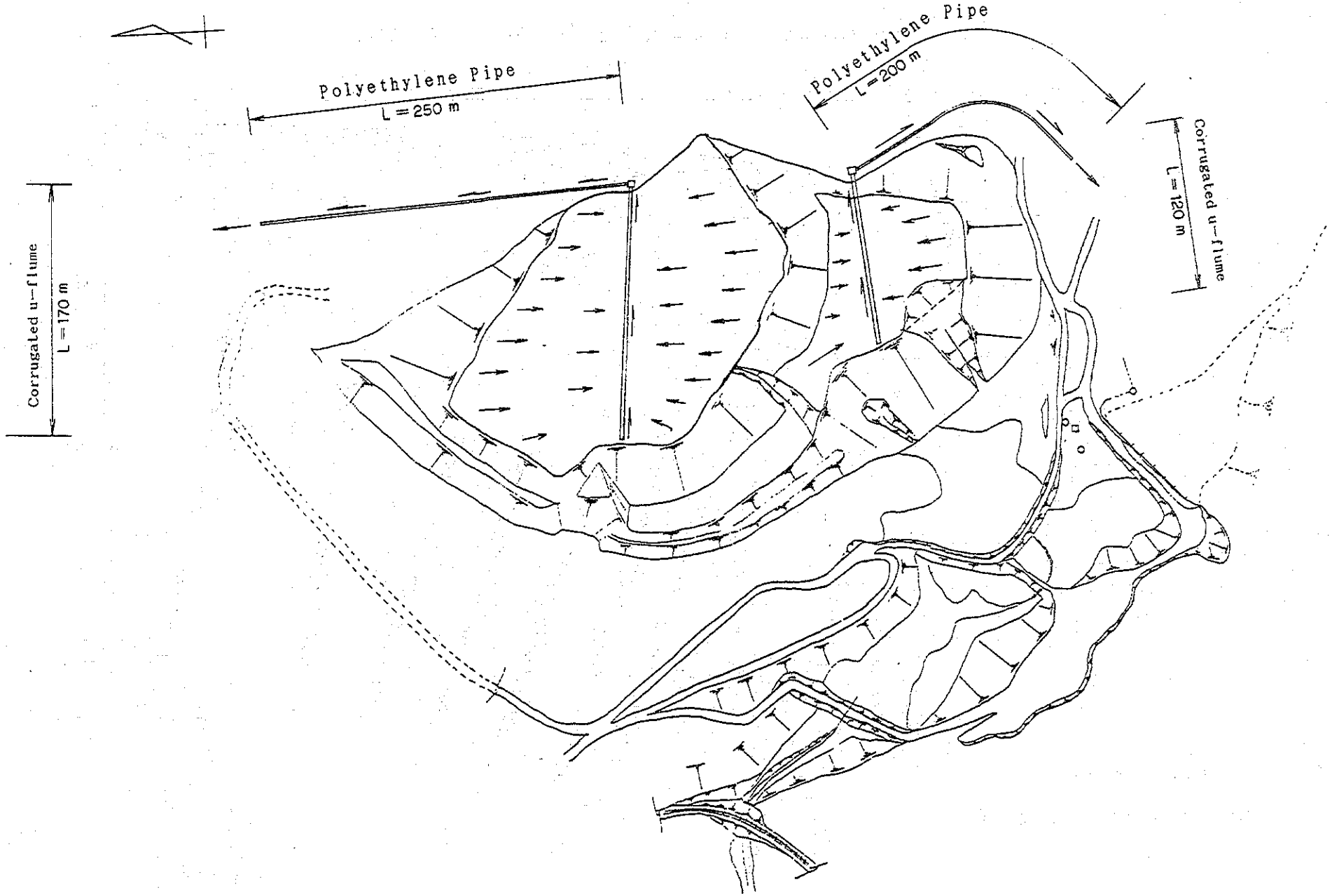

Fig. 3-9-7 Drainage Plan

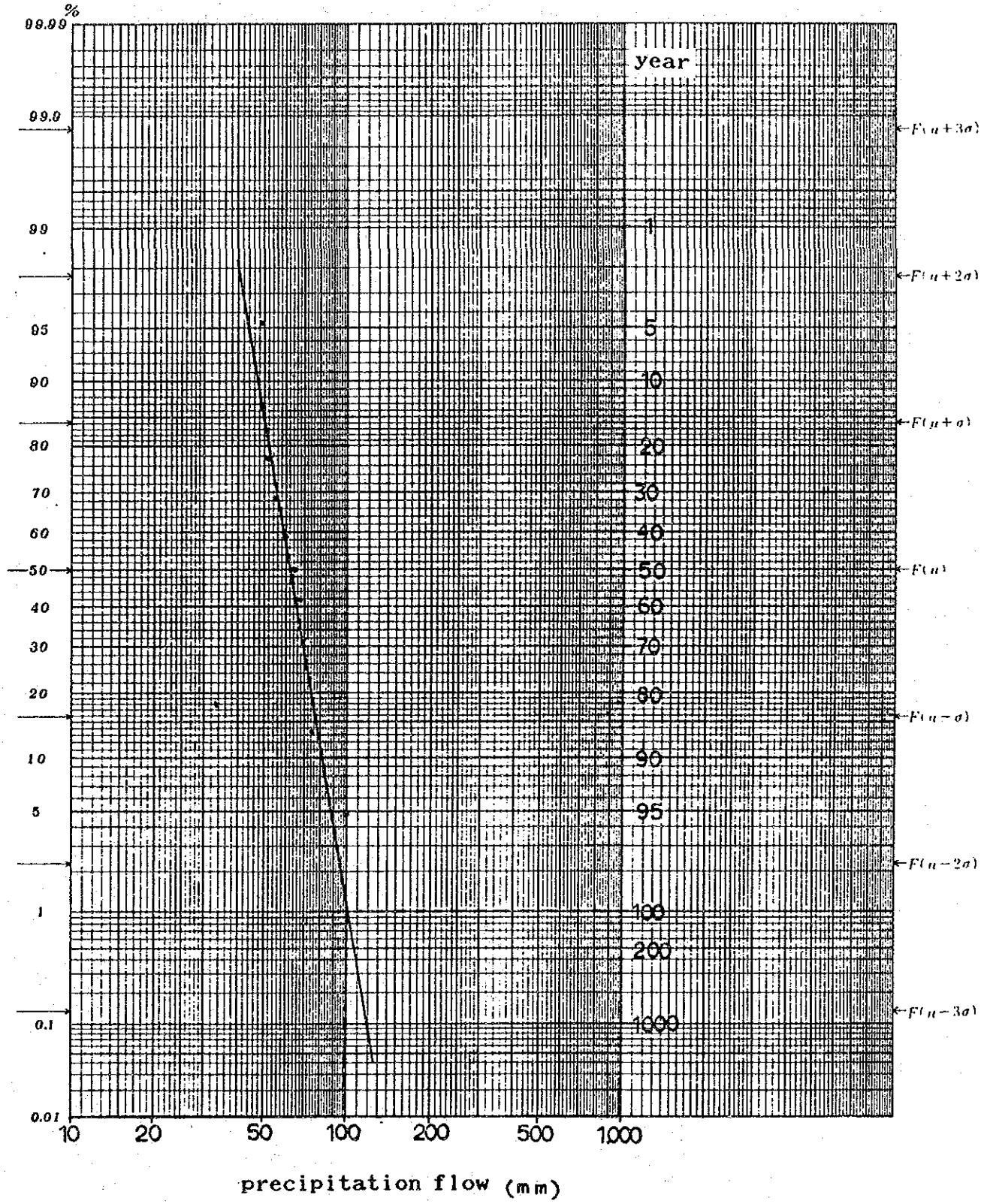

Fig. 3-9-8 Probability Precipitation

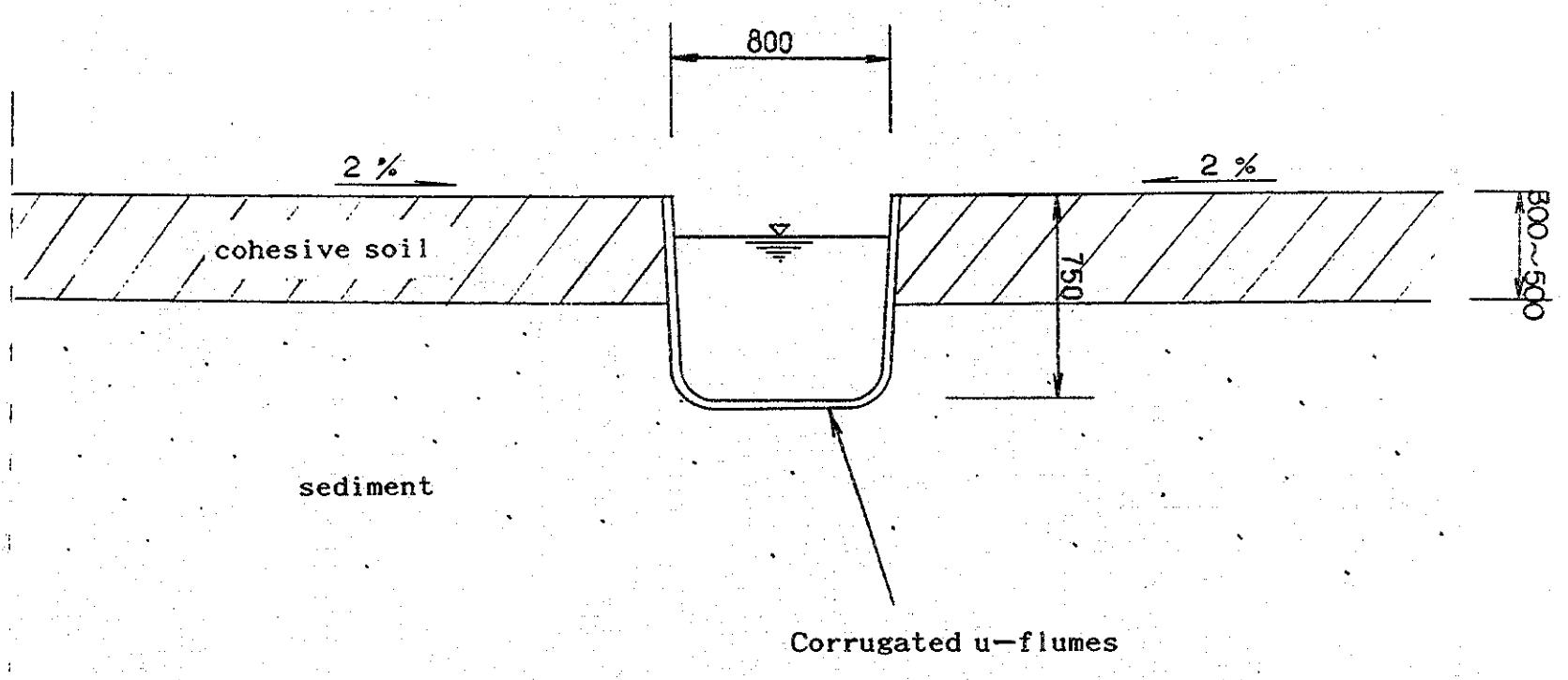

Fig. 3-9-9 Typical Cross Section of Drainage

Table 3-4-1 Hydrologic Measurement of Surface Water (El Bote)

Site	Season	Date	Section of Flow (m^2)	Velocity (m/sec)	Flow Rate (m^3/sec)	Daily Flow (m^3/day)
No. 0	Rainy	12, Aug.	0.16	0	0	0
No. 1	Dry	20, Mar.	0.0480	0.2122	1.019×10^{-2}	880.4
	Rainy	13, Aug.	0.0578	0.0896	5.177×10^{-3}	447.3
No. 2	Dry	20, Mar.	0	0	0	0
	Rainy	13, Aug.	0.0114	0.2313	2.631×10^{-3}	227.3
No. 3	Dry	20, Mar.	0.0112	0	0	0
	Rainy	12, Aug.	0.0127	0.0477	6.042×10^{-3}	522.0
No. 4	Dry	20, Mar.	0.0590	0.2380	1.404×10^{-2}	1,213.1
	Rainy	12, Aug.	0.0795	0.1767	1.405×10^{-2}	1,213.9
No. 5	Dry	20, Mar.	0.0318	0.2082	0.662×10^{-2}	572.0
	Rainy	12, Aug.	0.0735	0.1909	1.403×10^{-2}	1,212.3
No. 6	Dry	20, Mar.	0.0450	0.1051	0.473×10^{-2}	408.7
	Rainy	12, Aug.	0.0513	0.1048	5.372×10^{-3}	464.2

Table 3-4-2 Background and Water Supply Ceiling of Chemical Components in Water

(ppm)

Background Value	Cu	Pb	Zn	Fe	Cd	Total Cr	As	Hg	Cr^{6+}	CN
Fresh Water	0.003	0.003	0.020	0.1	0.032×10^{-3}	0.001	0.002	0.07×10^{-3}	0.001	0
Water Supply Ceiling	1	0.05	5	0.3	0.01	0.05	0.05	0.002	0.05	0

after Rose, W., Hawkes, H.E., and Webb, J.S. (1979): Geochemistry in Mineral Exploration
Water Supply Ceiling is by U.S. Enviromental Protection Agency (1977)

Table 3-4-3 Chemical Analysis of Surface Water (El Bote)

Site	Season	Date	Cu (ppm)	Pb (ppm)	Zn (ppm)	Fe (ppm)	Cd (ppm)	Total Cr (ppm)	As (ppm)	Hg (ppm)	Cr^{6+} (ppm)	CN (ppm)	pH
B-R1	Dry	20, Mar.	0.37	0.019	4.9	1.9	0.09	n.d.	n.d.	n.d.	n.d.	n.d.	7.93
	Rainy	13, Aug.	0.037	0.32	4.9	0.68	0.13	n.d.	0.003	0.0002	n.d.	n.d.	7.89
B-R2	Dry	20, Mar.	240	1.5	7,800	910	55	0.33	5.2	0.0004	n.d.	n.d.	2.54
	Rainy	12, Aug.	85	0.54	1,100	190	12	0.11	0.29	n.d.	n.d.	n.d.	2.56
B-R3	Dry	20, Mar.	0.03	1.0	6.5	0.31	0.12	0.009	0.03	n.d.	n.d.	n.d.	7.94
	Rainy	12, Aug.	0.005	n.d.	2.1	0.23	0.076	n.d.	0.003	0.0001	n.d.	n.d.	8.18
B-R4	Dry	20, Mar.	0.011	0.06	3.3	0.53	0.09	0.013	0.01	n.d.	n.d.	n.d.	8.15
	Rainy	12, Aug.	0.036	0.015	3.9	0.40	0.11	0.003	0.002	n.d.	n.d.	n.d.	7.76
B-R5	Dry	20, Mar.	0.33	0.09	5.3	1.4	0.12	0.02	0.003	n.d.	n.d.	n.d.	8.10
	Rainy	12, Aug.	0.019	0.002	3.2	0.54	0.11	n.d.	0.001	0.0004	n.d.	n.d.	7.75
B-R6	Rainy	12, Aug.	0.030	0.003	4.3	1.6	0.11	n.d.	0.008	n.d.	n.d.	n.d.	7.77
B-R7	Rainy	13, Aug.	0.059	0.022	3.9	1.7	0.065	0.001	n.d.	n.d.	n.d.	n.d.	7.72
B-D1	Dry	20, Mar.	0.06	0.21	10.4	1.2	0.21	0.04	0.003	n.d.	n.d.	n.d.	7.51
	Rainy	13, Aug.	0.092	0.37	6.9	1.3	0.25	0.055	n.d.	0.0011	n.d.	n.d.	7.77
B-W1	Rainy	13, Aug.	0.19	0.60	1.7	2.5	0.11	0.065	n.d.	n.d.	n.d.	n.d.	7.43

Electric Conductivity (μs/cm) is;
B-R1(Dry)=35, B-R1(Rainy)=58, B-R2(Dry)=240, B-R2(Rainy)=150,
B-R3(Dry)=43, B-R3(Rainy)=40, B-R5(Dry)=42, B-R5(Rainy)=40,
B-R6(Rainy)=38, B-R7(Rainy)=55, B-D1(Dry)=85, B-D1(Rainy)=60,
B-W1(Rainy)=82

R:River, D:Tailing Dam, W:Waste Water

Table 3-4-4 Micro Flow Measurement Data (El Bote B-1)

Depth (m)	Time (sec)	Impellor Count	Flow Direction	Velocity (cm/sec)
6.73	60	0	Up-flow	0.40
7.23	60	0	Up-flow	0.40

DATE 13 AUG 1991
TIME 09:58:53 AM
HOLE No.=B-1
WATER LEVEL=6.23m

Depth (m)	Time (sec)	Impellor Count	Flow Direction	Velocity (cm/s)
6.78	60	0	Up-flow	0.40
7.28	60	0	Up-flow	0.51

DATE 15 AUG 1991
TIME 11:59:13 AM
HOLE No.=B-1
WATER LEVEL=6.28m

DEPTH=10m

Table 3-4-4 Micro Flow Measurement Data (El Bote B-2)

Depth (m)	Time (sec)	Impellor Count	Flow Direction	Velocity (cm/sec)
7.76	60	0	Up-flow	0.40
8.76	60	0	Up-flow	0.40
9.76	60	0	Up-flow	0.40
10.76	60	1	Up-flow	0.51
11.76	60	0	Up-flow	0.40
12.76	60	0	Up-flow	0.40
13.76	60	0	Up-flow	0.40
14.76	60	1	Up-flow	0.51
15.76	60	0	Up-flow	0.40
16.76	60	0	Up-flow	0.40
17.76	60	0	Up-flow	0.40
18.76	60	0	Up-flow	0.40
19.76	60	0	Up-flow	0.40
20.76	60	0	Up-flow	0.40
21.76	60	0	Up-flow	0.40
22.76	60	0	Up-flow	0.40
23.76	60	0	Up-flow	0.40
24.76	60	0	Up-flow	0.40
25.76	60	0	Up-flow	0.40
26.76	60	0	Up-flow	0.40
27.76	60	0	Up-flow	0.40
28.76	60	0	Up-flow	0.40

DATE 12 AUG 1991
TIME 11:50:06 AM
HOLE No.=B-2
WATER LEVEL=6.76m
DEPTH=30m

Depth (m)	Time (sec)	Impellor Count	Flow Direction	Velocity (cm/sec)
7.83	60	2	Up-flow	0.63
8.83	60	0	Up-flow	0.40
9.83	60	6	Up-flow	1.11
10.83	60	6	Up-flow	1.11
11.83	60	0	Up-flow	0.40
12.83	60	3	Up-flow	0.75
13.83	60	1	Up-flow	0.51
14.83	60	0	Up-flow	0.40
15.83	60	0	Up-flow	0.40
16.83	60	0	Up-flow	0.40
17.83	60	0	Up-flow	0.40
18.83	60	0	Up-flow	0.40
19.83	60	0	Up-flow	0.40
20.83	60	3	Up-flow	0.75
21.83	60	0	Up-flow	0.40
22.83	60	0	Up-flow	0.40
23.83	60	0	Up-flow	0.40
24.83	60	0	Up-flow	0.40
25.83	60	0	Up-flow	0.40
26.83	60	0	Up-flow	0.40
27.83	60	0	Up-flow	0.40

DATE 15 AUG 1991
TIME 10:41:53 AM
HOLE No.=B-2
WATER LEVEL=6.83m
DEPTH=30m

Table 3-4-4 Micro Flow Measurement Data (El Bote B-3)

Depth (m)	Time (sec)	Impellor Count	Flow Direction	Velocity (cm/sec)
5.36	60	0	Up-flow	0.40
6.36	60	0	Up-flow	0.40
7.36	60	0	Up-flow	0.40
8.36	60	4	Up-flow	0.87
9.36	60	2	Up-flow	0.63
10.36	60	0	Up-flow	0.40
11.36	60	15	Up-flow	2.17
12.36	60	13	Up-flow	1.93
13.36	60	0	Up-flow	0.40
14.36	60	15	Up-flow	2.17
15.36	60	0	Up-flow	0.40
16.36	60	1	Up-flow	0.51
17.36	60	9	Up-flow	1.46
18.36	60	0	Up-flow	0.40

DATE 12 AUG 91
TIME 10:19:24 AM
HOLE No.=B-3
WATER LEVEL=4.36m
DEPTH=20m

Depth (m)	Time (sec)	Impellor Count	Flow Direction	Velocity (cm/sec)
5.36	60	0	Up-flow	0.40
6.36	60	0	Up-flow	0.40
7.36	60	1	Up-flow	0.51
8.36	60	0	Up-flow	0.40
9.36	60	37	Up-flow	4.77
10.36	60	1	Up-flow	0.51
11.36	60	2	Up-flow	0.63
12.36	60	2	Up-flow	0.63
13.36	60	13	Up-flow	1.93
14.36	60	17	Up-flow	2.41
15.36	60	26	Up-flow	3.47
16.36	60	15	Up-flow	2.17
17.36	60	6	Up-flow	1.11
18.36	60	1	Up-flow	0.51

DATE 15 AUG 1991
TIME 09:57:51 AM
HOLE No.=B-3
WATER LEVEL=4.36m
DEPTH=20m

Table 3-4-5 Characteristic of Aquifer (El Bote)

Site	Season	Date	Elevation (m)	Thickness of Aquifer	Flow Rate (m/sec)	Flow in Bore Hole(m^3/day)	Width of Aquifer	Total Flow (m^3/day)
B-2	Dry	19, Apr.	2,308 to 2,310	2m	0.0040	34.6	250m	172,800
	Rainy	12, Aug.			0.0044	38.0		190,080
		15, Aug.			0.0071	61.3		306,720
	Dry	19, Apr.	2,315 to 2,320	5m	0.0048	103.7		518,400
	Rainy	12, Aug.			0.0040	86.4		432,000
		15, Aug.			0.0052	112.3		561,600
B-3	Dry	19, Apr.	2,302 to 2,314	12m	0.0073	378.4	—	—
	Rainy	12, Aug.			0.0093	482.1		
		15, Aug.			0.0150	777.6		

Table 3-4-6 Chemical Analysis of Groundwater (El Bote)

Site	Season	Date	Cu (ppm)	Pb (ppm)	Zn (ppm)	Fe (ppm)	Cd (ppm)	Total Cr (ppm)	As (ppm)	Hg (ppm)	Cr^{6+} (ppm)	CN (ppm)	pH
B-B1	Rainy	13, Aug.	0.039	0.065	0.43	0.89	0.006	0.012	0.002	n.d.	n.d.	n.d.	7.97
B-B2	Dry	20, Mar.	0.13	0.14	n.d.	1.3	n.d.	0.04	n.d.	n.d.	n.d.	n.d.	7.70
	Rainy	12, Aug.	0.015	0.080	0.52	2.8	0.007	0.010	n.d.	0.0003	n.d.	n.d.	7.33
B-B3	Dry	20, Mar.	0.11	0.27	n.d.	2.0	n.d.	0.05	n.d.	n.d.	n.d.	n.d.	7.48
	Rainy	12, Aug.	0.014	0.021	0.41	1.2	0.011	0.022	n.d.	0.0004	n.d.	n.d.	7.53
B-M1	Rainy	13, Aug.	0.042	0.12	1.7	0.65	0.17	0.031	n.d.	0.0016	n.d.	n.d.	7.52
B-M2	Rainy	14, Aug.	0.21	0.14	140	2.1	2.5	0.032	n.d.	0.0006	n.d.	n.d.	6.35
B-M3	Rainy	14, Aug.	0.071	0.11	3.9	1.6	0.13	0.043	n.d.	n.d.	n.d.	n.d.	7.30

B:Drilling Hole, M:Interior of Mine

Electric Conductivity (μs/cm) is;
B-B1(Dry)=30, B-B2(Dry)=38, B-B2(Rainy)=32, B-B3(Dry)=33,
B-B3(Rainy)=31, B-M1(Rainy)=40, B-M2(Rainy)=85, B-M3(Rainy)=48

Table 3-4-7 Permeability Coefficient Data

(El Bote)

Sample Number	BR-1	BR-2	BR-3	BR-4	BR-5
D 10(mm)	0.2600	0.1100	0.0065	0.0014	0.0014
D 60(mm)	2.0000	0.6500	0.1900	0.3900	0.5000
Uniformity Coeffcient	7.7	5.9	29.2	278.6	357.1
K (cm/sec) by Hazen's Formula	9.02E-02	1.61E-02	5.64E-05	2.61E-06	2.61E-06

K:Permeability Coefficient(cm/sec)

D10(mm):Particle-size(mm) on 10% Cumulative Curve = Effecitve Size(de)

Table 3-4-8 Permeability and Porosity Model

Legend No.	Matrix Permeabilty pkm(cm/sec)	Fracture Permeability pkf(cm/sec)	Fracture Zone Width hef(m)	Matrix Porosity porm(%)	Fracture Porosity porf(%)
1 (Vein)	10^{-3}	0	0	30	30
2 (Aquifer)	5×10^{-4}	10^{-2}	0	30	30
3 (Aquitard)	10^{-4}	10^{-3}	0	20	30
5 (Aquiclude)	10^{-6}	10^{-3}	0	15	30
7 (Aquifuge)	10^{-7}	10^{-3}	0	5	30

Model's Block Permeability(K) = (hef/△x)×pkf+(1-hef/△x)×pkm

△x = block width(m)

Table 3-5-1 Chemical Analysis of Soil

(El Bote) (ppm)

No.	Cu	Pb	Zn	Fe(wt%)	Cd	Sb	Cr	As	Hg
BS-1	140	740	1,900	2.6	13.0	20	35	120	0.28
BS-2	220	1,400	3,200	4.2	26.0	26	36	190	0.19
BS-3	470	560	940	3.6	9.0	62	55	74	0.87
BS-4	33	100	130	2.7	2.4	50	36	32	0.66
BS-B1	160	840	4,200	3.7	44.0	39	60	57	3.40
BS-B2	89	1,000	1,900	4.8	19.0	36	110	31	2.30
BS-B3	100	69	190	7.5	7.3	48	170	7	1.20
BS-B4	72	5,300	710	4.2	5.7	32	50	40	1.70
BS-B5	110	130	310	8.3	8.1	42	140	21	1.80
BS-B6	57	120	210	6.7	7.1	68	220	9	1.10
BS-B7	88	94	100	4.9	1.6	61	87	16	1.00
BS-B8	37	67	200	3.2	4.2	28	31	18	0.73
BS-B9	110	98	220	2.7	3.8	35	37	23	0.98
BS-B10	31	83	200	3.2	3.9	37	37	8	1.30

(Background in Soil) (ppm)

Elemnts	Cu	Pb	Zn	Fe(wt%)	Cd	Sb	Cr	As	Hg
Background	15	17	36	2.1	0.5	2	43	7.5	0.056

by Rose, A.T. et al. (1979):Geochemistry in Mineral Exploration, Academic Press, 657P.

Table 3-6-1 Soil Test Quantity

Dry Season		Rainy Season	
No.	Depth(m)	No.	Depth(m)
BD-1	0.0- 0.6 5.0- 5.6 10.0-10.6 15.0-15.6 20.0-20.6	S-1 S-2 S-3 S-4	0.5- 1.0 0.8- 1.2 0.6- 1.2 0.5- 1.0
BD-2	0.0- 0.6 5.0- 5.6 10.0-10.6 15.0-15.6		
D-1	0.8- 1.0 1.5- 1.7		
D-2	0.8- 1.0 1.5- 1.7		
D-3	0.8- 1.0 1.5- 1.7		
D-4	0.8- 1.0 1.5- 1.7		
D-5	0.8- 1.0 1.5- 1.7		
Total	19 samples	Total	4 samples

Table 3-6-2 Soil Test Data

(Dry Season)

Sample No.	BD－1					BD－2			
Depth (m)	0.0～0.6	5.0～5.6	10.0～10.6	15.0～15.6	20.0～20.6	0.0～0.6	5.0～5.6	10.0～10.6	15.0～15.6
Water Content (%)	10.0	9.7	11.3	3.5	2.3	16.2	15.0	13.7	20.3
Specific Gravity	2.59	2.62	2.60	2.64	2.61	2.62	2.63	2.60	2.60
Wet Density (g/cm³)	1.573	1.496	1.632	1.593	1.521	1.594	1.630	1.575	1.485
Liquid Limit (%)	24.0	30.0	25.0	26.2	23.0	24.7	22.0	24.0	25.7
Plastic Limit (%)	21.0	19.0	20.0	17.8	20.0	19.5	20.0	20.0	12.6
Angle of Internal Fliction (°)	34.0	36.5	32.0	35.0	31.5	26.5	28.0	25.0	22.5
Cohesion (tf/m²)	0.0	0.0	0.0	0.0	0.0	1.0	2.0	0.5	1.0
Coefficient of Permeability (cm/sec)	3.01 $\times10^{-3}$	4.88 $\times10^{-3}$	3.24 $\times10^{-3}$	2.85 $\times10^{-3}$	3.13 $\times10^{-3}$	1.06 $\times10^{-3}$	3.35 $\times10^{-4}$	9.84 $\times10^{-5}$	9.79 $\times10^{-5}$

(dry season)

Sample No.	D－1		D－2		D－3		D－4		D－5	
Depth (m)	0.8～1.0	1.5～1.7	0.8～1.0	1.5～1.7	0.8～1.0	1.5～1.7	0.8～1.0	1.5～1.7	0.8～1.0	1.5～1.7
Water Content (%)	16.7	13.4	14.3	15.3	14.6	18.4	8.7	6.5	7.2	9.1
Spefcific Gravity	2.66	2.63	2.63	2.60	2.62	2.65	2.61	2.61	2.62	2.60
Wet Density (g/cm³)	1.625	1.590	1.531	1.655	1.630	1.622	1.780	1.695	1.701	1.700
Liquid Limet (%)	22.3	26.0	20.4	34.3	31.0	25.0	38.0	41.0	40.2	39.0
Plastic Limit (%)	18.8	19.0	16.4	21.3	18.0	16.0	8.5	7.6	10.0	6.8
Angle of Internal Fliction (°)	21.0	23.0	22.6	24.5	20.5	25.0	19.5	21.0	23.2	19.0
Cohesion (tf/m²)	1.0	1.0	2.0	1.5	2.0	1.0	5.0	5.0	4.5	5.0
Coefficient of Permeability (cm/sec)	3.38 $\times10^{-5}$	3.35 $\times10^{-4}$	1.09 $\times10^{-5}$	4.07 $\times10^{-5}$	5.90 $\times10^{-5}$	1.35 $\times10^{-4}$	1.03 $\times10^{-5}$	1.21 $\times10^{-5}$	7.17 $\times10^{-6}$	8.71 $\times10^{-6}$

(Rainy season)

Sample No.	S－1	S－2	S－3	S－4
Depth (m)	1.0～1.5	1.0～1.5	1.0～1.5	1.0～1.5
Water Content (%)	36.9	33.5	36.7	14.8
Specific Gravity	2.64	2.61	2.64	2.61
Wet Density (g/cm³)	1.762	1.685	1.875	1.933
Liquid Limit (%)	37.6	38.2	42.4	23.1
Plastic Limit (%)	25.6	22.8	21.2	19.3
Angle of Internal Fliction (°)	25.3	20.6	25.6	31.8
Cohesion (tf/m²)	1.2	0.9	1.3	0.0
Coefficient of Permeability (cm/sec)	8.52 $\times10^{-5}$	12.65 $\times10^{-5}$	8.29 $\times10^{-5}$	3.95 $\times10^{-3}$

Table 3-6-3 Natural Moisture Content and Wet Density

	Tailing Dam	Tailing
Natural Water Content (W)	14.8 %	35.7 %
Wet Density(ρ_t)	1.933 g/cm^3	1.774 g/cm^3

Table 3-6-4 Consistency Data of Soil

	Tailing Dam	Tailing
Liquid Limit (L.L)	23.1 %	39.4 %
Plastic Limit (P.L)	19.3 %	23.2 %
Natural Water Content (W)	14.8 %	32.7 %
Plasticity Index (Ip)	3.8 %	16.2 %
Consistency Index (Ic)	2.2 %	0.4 %

Table 3-6-5 A Result of Tailing Dam Stability Analysis

Element		Ordinary Condition (Kh=0.00)	Earthquake Condition (Kh=0.15)
Center of Circular Arc	X(m)	50.00	50.00
	Y(m)	2388.00	2398.00
Radius R(m)		6.657	13.728
Resisting Moment MR(tf・m)		17.508	42.811
Sliding Moment MD(tf・m)		26.383	85.909
Safety Factor Fs=MR/MD		0.6636	0.4983

Table 3-7-1 Wind System Data

Times	Date (y.m.d.)		Wind Velocity Data (m/sec)			Wind Direction Data		
	Starting	Ending	Max.	Min	Average	Main Dir.	Count	Total Count
1	91. 3.15	91. 3.21	16.0	1.5	7.5	S W	88	127
2	91. 4.17	91. 5. 1	12.0	0.0	2.5	S	107	181
3	91. 5.19	91. 6.11	-	-	-	S E	109	259
4	91. 7.19	91. 7.25	-	-	-	S E	66	76

Table 3-7-2 Wind Speed Data

(El Bote in dry season) (m/sec)

Hour	3/15	3/16	3/17	3/18	3/19	3/20	3/21	Total	mean
0	-	6.0	6.0	2.5	4.0	7.0	4.3	29.8	5.0
1	-	6.5	6.5	3.0	3.5	6.8	5.2	31.5	5.3
2	-	9.0	7.0	3.0	4.0	3.8	4.5	31.3	5.2
3	-	9.0	6.5	1.5	3.0	3.8	5.0	28.8	4.8
4	-	9.0	5.0	1.5	1.5	5.5	5.5	28.0	4.7
5	-	8.0	6.5	1.5	1.5	5.0	6.5	29.0	4.8
6	-	10.5	7.0	3.5	2.3	5.0	7.0	35.3	5.9
7	-	11.5	7.5	3.5	4.0	6.0	8.0	40.5	6.8
8	-	11.0	7.5	1.5	1.5	6.3	7.0	34.8	5.8
9	-	12.0	9.0	1.5	2.5	7.8	8.0	40.8	6.8
10	-	10.0	9.0	1.5	5.0	10.0	9.0	44.5	7.4
11	-	12.0	8.5	3.0	5.5	11.3	10.3	50.6	8.4
12	-	12.0	9.5	6.0	7.8	13.0	13.5	61.8	10.3
13	-	13.5	9.5	5.0	10.0	13.0	14.5	65.5	10.9
14	-	12.0	10.0	6.3	10.0	13.5	16.0	67.8	11.3
15	-	13.0	11.0	7.8	10.0	13.3	15.0	70.1	11.7
16	-	13.0	11.5	8.0	9.8	13.0	13.6	68.9	11.5
17	-	11.0	10.5	6.8	9.3	11.5	12.5	61.6	10.3
18	13.0	10.5	9.8	7.5	8.3	12.0	12.0	73.1	10.4
19	10.5	10.5	7.5	6.3	8.0	8.8	10.0	61.6	8.8
20	5.0	9.0	4.5	5.0	6.3	7.0	12.0	48.8	7.0
21	5.5	9.0	4.5	4.5	5.0	5.5	6.0	40.0	5.7
22	8.0	7.5	2.0	3.5	4.5	6.3	11.5	43.3	6.2
23	7.0	6.0	3.0	2.0	5.8	3.8	7.8	35.4	5.1
Total	49	242	179	96	133	199	225	1123	160
Count	7	24	24	24	24	24	24	151	21.6
Mean	7.0	10.1	7.5	4.0	5.5	8.3	9.4	52	7.5
Max.	13.0	13.5	11.5	8.0	10.0	13.5	16.0	86	12.1
Min.	0.0	6.0	2.0	1.5	1.5	3.8	4.3	19	3.2

(El Bote in rainy season) (m/sec)

Hour	4/17	4/18	4/19	4/20	4/21	4/22	4/23	4/24	4/25	4/26	4/27	4/28	4/29	4/30	5/1	Total	mean
0	2.0	2.0	2.5	7.5	7.5	0.0	2.0	0.0	3.5	6.5	5.0	6.5	6.0	4.0	4.0	59.0	3.9
1	1.5	1.0	4.0	2.5	6.5	3.0	2.5	0.0	4.5	6.5	6.0	7.5	5.5	5.5	3.5	60.0	4.0
2	2.0	1.0	4.5	6.0	5.0	2.5	1.5	3.0	4.5	6.0	7.5	8.0	6.0	5.0	5.0	67.5	4.5
3	2.5	1.0	2.5	6.5	5.0	2.5	4.5	2.0	5.0	6.0	7.5	7.5	5.0	5.0	5.0	67.5	4.5
4	1.5	3.0	1.0	7.0	6.0	2.5	4.5	2.5	5.5	5.5	8.0	7.5	5.0	3.5	4.5	67.5	4.5
5	4.0	3.0	3.0	7.5	5.0	2.0	2.5	3.0	4.5	5.0	7.5	3.0	5.5	3.5	5.0	64.0	4.3
6	7.5	1.5	4.0	6.5	1.5	1.5	2.5	2.0	3.5	6.0	7.5	3.5	4.5	4.5	3.5	60.0	4.0
7	4.5	2.5	6.0	0.0	5.5	0.5	0.5	2.5	2.5	7.0	5.0	0.0	2.0	2.5	2.5	43.5	2.9
8	0.0	0.0	0.0	0.0	0.0	0.5	0.0	1.0	4.0	6.0	6.0	0.0	1.0	0.0	5.5	24.0	1.6
9	0.0	0.0	0.0	0.0	0.0	0.0	0.0	0.0	0.0	0.0	9.0	0.0	0.0	0.0	5.0	14.0	0.9
10	0.0	0.0	0.0	0.0	0.0	0.0	0.0	0.0	0.0	0.0	7.5	0.0	0.0	0.0	6.0	13.5	0.9
11	0.0	0.0	0.0	0.0	0.0	0.0	0.0	0.0	0.0	0.0	7.0	0.0	0.0	0.0	5.0	12.0	0.8
12	0.0	0.0	0.0	0.0	0.0	0.0	0.0	0.0	0.0	0.0	6.5	0.0	0.0	0.0	5.5	12.0	0.8
13	0.0	0.0	0.0	0.0	0.0	0.0	0.0	0.0	0.0	0.0	7.0	0.0	0.0	0.0	6.0	13.0	0.9
14	0.0	0.0	0.0	0.0	0.0	0.0	0.0	0.0	0.0	0.0	10.0	0.0	0.0	0.0	5.5	15.5	1.0
15	0.0	0.0	0.0	0.0	0.0	0.0	0.0	0.0	0.0	0.0	11.0	0.0	0.0	0.0	5.5	16.5	1.1
16	0.0	0.0	0.0	0.0	0.0	0.0	0.0	0.0	0.0	0.0	12.0	0.0	0.0	0.0	0.0	12.0	0.8
17	0.0	0.0	0.0	0.0	0.0	0.0	0.0	0.0	0.0	0.0	0.0	0.0	0.0	0.0	0.0	0.0	0.0
18	0.0	0.0	0.0	0.0	0.0	0.0	0.0	0.0	0.0	0.0	0.0	0.0	0.0	0.0	0.0	0.0	0.0
19	0.0	5.0	7.5	0.0	0.0	0.0	0.0	0.0	0.0	0.0	0.0	0.0	0.0	0.0	0.0	12.5	0.8
20	5.0	5.0	5.5	5.0	0.0	3.0	0.0	5.0	0.0	8.0	9.0	7.5	4.0	5.0	4.0	66.0	4.4
21	3.0	5.0	8.0	8.0	0.0	3.0	0.0	4.5	6.5	6.0	8.5	10.0	4.5	4.0	3.0	74.0	4.9
22	3.5	2.5	7.5	8.0	0.0	3.0	0.0	2.5	6.0	5.5	8.0	7.5	4.0	3.0	3.0	64.0	4.3
23	2.5	2.5	7.5	8.0	0.0	3.5	0.0	3.5	7.0	5.5	7.0	7.5	3.5	3.5	4.0	65.5	4.4
Total	39.5	35.0	63.5	72.5	42.0	27.5	20.5	31.5	57.0	79.5	163	76.0	56.5	49.0	91.0	904	60.2
Count	24	24	24	24	24	24	24	24	24	24	24	24	24	24	24	360	24
Mean	1.6	1.5	2.6	3.0	1.8	1.1	0.9	1.3	2.4	3.3	6.8	3.2	2.4	2.0	3.8	37.6	2.5
Max.	7.5	5.0	8.0	8.0	7.5	3.5	4.5	5.0	7.0	8.0	12.0	10.0	6.0	5.5	6.0	104	6.9
Min.	0.0	0.0	0.0	0.0	0.0	0.0	0.0	0.0	0.0	0.0	0.0	0.0	0.0	0.0	0.0	0.0	0.0

Table 3-7-3 Wind Direction Data

(El Bote in dry season)

Direction	3/15	3/16	3/17	3/18	3/19	3/20	3/21	Total
N	0	0	0	2	0	0	0	2
NW	0	0	0	1	0	0	0	1
W	0	0	0	4	0	0	0	4
SW	5	11	5	9	11	9	5	55
S	2	13	19	8	9	13	17	81
SE	0	0	0	0	4	3	2	9
E	0	0	0	0	0	0	0	0
NE	0	0	0	0	0	0	0	0
Count	7	24	24	24	24	25	24	152
Main Dir.	SW	S	S	SW	SW	S	S	S

(El Bote in rainy season)

Direction	4/17	4/18	4/19	4/20	4/21	4/22	4/23	4/24	4/25	4/26	4/27	4/28	4/29	4/30	5/1	Total
N	0	1	10	1	0	0	0	0	0	0	0	0	0	0	0	12
NW	0	5	2	0	0	0	4	0	0	0	0	0	0	0	0	11
W	1	2	1	0	0	3	2	1	0	0	0	0	0	0	0	10
SW	3	4	0	2	0	4	1	6	0	0	8	0	0	0	4	32
S	5	1	0	0	2	5	1	4	12	13	13	11	12	12	16	107
SE	3	0	0	0	5	0	0	0	0	0	0	0	0	0	0	8
E	0	0	0	8	1	0	0	0	0	0	0	0	0	0	0	9
NE	0	0	0	0	0	0	0	0	0	0	0	0	0	0	0	0
Count	12	13	13	11	8	12	8	11	12	13	21	11	12	12	12	181
Main Dir.	S	NW	N	E	SE	S	NW	SW	S	S	S	S	S	S	S	S

(El Bote in rainy season)

Direction	5/19	5/20	5/21	5/22	5/23	5/24	5/25	5/26	5/27	5/28	5/29	5/30	5/31	6/ 1	6/ 2	6/ 3	6/ 4	6/ 5	6/ 6	6/ 7	6/ 8	6/ 9	6/10	6/11	Total
N	0	0	1	0	0	0	1	2	2	0	0	0	0	0	0	4	4	1	1	0	2	0	0	0	18
NW	0	0	3	0	0	0	1	2	0	0	0	0	0	0	0	3	0	0	0	0	0	0	0	0	9
W	0	1	0	0	0	0	2	1	0	0	0	0	0	1	1	1	0	0	0	0	0	0	0	0	7
SW	0	1	1	0	4	3	1	1	0	0	0	1	1	4	5	0	0	0	0	0	0	0	0	0	22
S	1	2	4	8	7	8	3	0	2	0	0	2	6	5	0	0	0	0	0	0	0	0	2	0	50
SE	8	4	2	3	0	5	5	6	5	10	8	9	3	1	1	1	3	8	6	1	7	4	4	5	109
E	2	1	0	0	0	0	2	3	1	0	2	0	0	0	3	1	0	1	3	8	1	7	1	0	36
NE	0	3	0	0	0	0	0	0	1	0	0	0	0	0	0	0	2	0	0	2	0	0	0	0	8
Count	11	12	11	11	11	16	15	15	11	10	10	12	10	11	10	10	9	10	10	11	10	11	7	5	259
Main Dir.	SE	SE	S	S	S	S	SE	SE	SE	SE	SE	SE	SE	S	S	N	N	SE	SE	E	SE	E	SE	SE	SE

(El Bote in rainy season)

Direction	7/19	7/20	7/21	7/22	7/23	7/24	7/25	Total
N	0	0	0	0	0	0	0	0
NW	0	0	0	0	0	0	0	0
W	0	0	0	0	0	0	0	0
SW	0	0	0	0	0	0	0	0
S	0	1	0	0	1	0	0	2
SE	12	10	11	7	10	11	5	66
E	0	1	1	0	0	0	6	8
NE	0	0	0	0	0	0	0	0
Count	12	12	12	7	11	11	11	76
Main Dir.	SE	SE	SE	SE	SE	SE	SE	SE

Table 3-7-4 Dust Jar Measurement Data

St	Start time	End time	Dust Weight(mg)*1	Dust Weight(mg)*2	pH
BD-1	3/15 14:50	3/21 12:00	21.2	693.2	7.1
BD-2	3/15 15:40	3/21 10:40	15.9	16.9	7.3
BD-3	3/15 16:20	3/21 10:20	15.3	16.3	7.3
BD-4	3/15 16:55	3/21 13:30	11.3	79.3	7.4
BD-5	3/15 17:10	3/21 11:40	10.5	53.5	7.6
BD-6	3/15 18:00	3/21 10:00	8.8	127.8	7.3

*1 Dust Weight of Insolble Components (mg)

*2 Dust Weight of Soluble Components (mg)

Table 3-7-5 Chemical Analysis of Falling Dust

Chemical Composition of the Dust Samples

sample Number	SiO2 (%)	Al (%)	Fe (%)	Ca (%)	Na (%)	Cu (ppm)	Pb (ppm)	Zn (ppm)	Cd (ppm)
BD-1	66	3.1	3.2	0.15	0.14	800	740	1,900	20
BD-4	77	2.7	3.6	0.49	0.17	320	2,400	4,400	33
BD-5	65	2.8	3.3	0.33	0.16	530	1,700	3,800	27
Standard	61	15.6	5	5.17	3.91	55	15	70	0.2

The Ratio of Chemical Composition to Al Contents in the Samples

Sample Number	SiO2/Al	Al/Al	Fe/Al	Ca/Al	Na/Al	Cu/Al ×10000	Pb/Al ×10000	Zn/Al ×10000	Cd/Al ×10000
BD-1	21.29	1.00	1.03	0.05	0.05	258.1	238.7	612.9	6.45
BD-4	28.52	1.00	1.33	0.18	0.06	118.5	888.9	1629.6	12.22
BD-5	23.21	1.00	1.18	0.12	0.06	189.3	607.1	1357.1	9.64
Standard	3.91	1.00	0.32	0.33	0.25	3.5	1.0	4.5	0.01

The Caluculation of the Heavy Metal Enrich Ratio

Sample Number	Cu	Pb	Zn	Cd
BD-1	74	249	136	645
BD-1	34	926	362	1222
BD-1	54	632	302	964

Table 3-7-6 Condition of Low Volume Air Sampler

Starting Time	Ending Time	Running Time	Absorption Ratio (l/min)	Absorption Volume (l)
90.3.18 10:45	90.3.20 17:10	54.45hrs.	15	48,975

Table 3-7-7 Low Volume Air Sampler Measurement Data

Sample Weight (mg)	Concentration of Particles in Atmosphere (mg/m3)
2.0	0.041

Table 3-7-8 Digital Type Dust Monitor Data (1)

(mg/m3)

Site No.	15/Mar	16/Mar	17/Mar	18/Mar	19/Mar	20/Mar	21/Mar	Mean
1	-	0.038	0.037	0.038	-	-	-	0.038
2	-	0.039	0.038	0.038	-	-	-	0.038
3	0.042	0.040	0.038	-	-	-	0.036	0.039
4	-	0.039	0.038	-	0.058	-	-	0.045
5	0.039	0.038	0.038	-	0.036	-	0.036	0.037
6	-	0.039	0.039	-	-	-	-	0.039
7	-	0.038	0.037	-	-	-	-	0.038
8	0.048	0.038	0.037	0.037	-	-	0.034	0.039
9	-	0.038	0.037	-	-	-	-	0.038
10	-	0.040	0.038	0.039	0.043	0.049	0.039	0.041
11	0.048	0.055	0.038	0.038	0.040	0.053	0.038	0.044
12	0.175	0.064	0.041	0.039	0.036	0.099	0.097	0.079
13	-	-	-	0.038	0.049	0.066	-	0.051
14	-	-	-	0.038	0.043	0.062	-	0.048
15	-	-	-	0.038	0.038	0.065	-	0.047
16	-	-	-	0.038	0.039	0.050	-	0.042
17	-	-	-	0.038	0.038	0.048	-	0.041
18	-	-	-	0.038	0.038	0.050	-	0.042
19	0.043	0.046	0.035	0.037	0.038	0.069	0.037	0.044
20	-	-	-	0.037	-	-	-	0.037
21	-	-	-	0.037	-	-	-	0.037
22	-	0.041	0.039	0.038	-	0.045	-	0.041
23	-	0.071	0.040	-	-	-	-	0.056
24	-	0.111	0.037	-	-	-	-	0.074
25	-	0.075	0.038	-	-	-	-	0.057
26	-	0.059	0.038	-	-	-	-	0.048
27	-	0.059	0.042	-	-	-	-	0.051
28	-	0.092	0.045	-	-	-	-	0.069
29	-	-	-	0.038	0.040	0.057	0.040	0.039
30	-	-	-	0.038	0.040	0.055	0.038	0.039
31	-	-	-	0.039	0.043	0.055	0.061	0.041
32	-	-	-	0.040	0.037	0.091	0.040	0.051
33	-	-	-	0.040	0.036	0.091	0.061	0.038
34	-	-	-	0.040	0.038	0.073	0.053	0.039
35	-	-	-	0.040	0.040	0.067	-	0.040
36	-	-	-	0.040	0.040	0.065	-	0.040

Table 3-7-8 Digital Type Dust Monitor Data (2)

(El Bote in Dry Season) (cpm)

Site No.	15/Mar	16/Mar	17/Mar	18/Mar	19/Mar	20/Mar	21/Mar	Mean
1	-	18	18	19	-	-	-	18
2	-	19	18	19	-	-	-	19
3	21	19	19	-	-	-	17	19
4	-	19	19	-	28	-	-	22
5	19	19	19	-	17	-	17	18
6	-	19	19	-	-	-	-	19
7	-	19	18	-	-	-	-	18
8	23	19	18	18	-	-	17	19
9	-	18	18	-	-	-	-	18
10	-	19	19	19	21	24	19	20
11	23	27	19	18	20	26	19	22
12	85	31	20	19	18	48	47	38
13	-	-	-	19	24	32	-	25
14	-	-	-	19	21	30	-	23
15	-	-	-	19	19	31	-	23
16	-	-	-	19	19	24	-	21
17	-	-	-	19	18	23	-	20
18	-	-	-	19	19	24	-	21
19	21	23	17	18	19	29	18	21
20	-	-	-	18	-	-	-	18
21	-	-	-	18	-	-	-	18
22	-	20	19	19	-	22	-	20
23	-	35	20	-	-	-	-	27
24	-	54	18	-	-	-	-	36
25	-	37	19	-	-	-	-	28
26	-	29	18	-	-	-	-	23
27	-	29	21	-	-	-	-	25
28	-	45	22	-	-	-	-	34
29	-	-	-	19	20	28	20	21
30	-	-	-	19	20	27	19	21
31	-	-	-	19	21	27	30	24
32	-	-	-	19	18	45	20	26
33	-	-	-	19	18	45	30	28
34	-	-	-	19	19	36	26	25
35	-	-	-	19	20	33	-	24
36	-	-	-	19	19	32	-	24

Table 3-7-9 Comparative Data of Digital Type Dust Monitors

Date	Counting Time (Min.)	Dust Monitor Serial Numbers				
		1100754	1100762	1100766	1100768	1100774
15/Mar	30	0.993	1.259	1.010	1.159	1.000
16/Mar	12	0.944	1.272	1.046	1.174	1.000
17/Mar	10	0.998	1.267	1.030	1.126	1.000
18/Mar	10	1.052	1.263	1.013	1.078	1.000
19/Mar	15	1.039	1.280	1.014	1.093	1.000
20/Mar	25	1.121	1.338	0.921	1.149	1.000
21/Mar	10	1.117	1.335	0.924	1.149	1.000

Table 3-9-1 A Result of Tailing Dam Stability Analysis

Element		Ordinary Condition (Kh=0.00)	Earthquake Condition (Kh=0.15)
Center of Circular Arc	X(m)	100.00	100.00
	Y(m)	2435.0	2435.0
Radius R(m)		24.0	24.0
Resisting Moment MR(tf・m)		840.456	797.318
Sliding Moment MD(tf・m)		448.808	623.934
Safety Factor Fs=MR/MD		1.8726	1.2779

Table 3-9-2 Day Probability Precipitation

Order i	Date	Precipitation (mm)	$\frac{2i-1}{2N}$ x100
1	1983.8.21	98.1	4.55
2	1990.8.23	83.8	13.64
3	1983.8. 8	81.8	22.73
4	1991.7.12	79.7	31.82
5	1984.7.11	76.1	40.91
6	1986.7.13	73.5	50.00
7	1988.6.14	69.4	59.09
8	1981.6.15	64.7	68.18
9	1985.6.26	61.8	77.27
10	1982.7. 1	58.5	86.36
11	1989.8.21	49.7	95.45

4. Survey Results and Countermeasures in the Area of Parral

4. SURVEY RESULTS AND COUNTERMESURES IN THE AREA OF PARRAL

4-1 General Situation

4-1-1 Location, topography and climate

Parral mineral processing plant is located 5km west of Hidalgo del Parral, southern end of the State of Chihuahua. It is about 1,800m above the sea level. Average temperature throughout a year is 14 ~ 15° C but goes down to 5° C in the winter season. The rainy season starts in May and runs till September for five months. The rest is almost dry. Annual rainfall averages 600mm. Throughout the dry season the west wind blows hard.

4-1-2 Outline of the plant

Parral plant was started in 1967 by an union type organization and then has been operated by CFM since 1983.

The State of Chihuahua stands the first place in mining production of the United Mexican States. It ranks the top position in production of Ag,Pb and Zn, and the second in Cu. In Parral area are located about 30 medium and small size metal mines producing Au, Ag, Pb and Zn. The Parral plant purchases these crude ores to process them by the following two different circuits. Thus, Pb and Zn concentrates are recovered by flotation from the sulphide ores and Au-Ag precipitate through cyanidation from the oxide ores. Capacity of the flotation and cyanidation plants are 400 and 240 tons a day respectively.

In the flotation plant bulk or differential flotation method is employed depending upon metal contents in the crude ore, just like El Bote plant. In case of differential flotation about 200kg of sodium cyanide (NaCN) is added per month into the flotation pulp. Cyanidation is operated intermittently, also depending on metal values and other conditions. when in operation considerable amount of NaCN, 1,500 ~ 2,000kg per month is added into the circuit. This could seriously affect on environmental water pollution.

In the tailing dam a large volume of slime(waste) material containing cyanide have been dumped for long. It is urgent to take some countermeasures to prevent these waste materials and effluent from flowing into nearby rivers.

Water consumption in the plant is about 600m^3 a day, of which 400m^3 is

supplied as fresh water from the underground mine and the rest is recycled from the flotation tailing by recovering as thickener overflow.

4-2 Geology

4-2-1 Outline of geology

The survey area is located in the Upland on the slope of the Sierra Madre Occidental, in the southern Chihuahua State. The area is about 190km south from the city of Chihuahua, the capital of Chihuahua state. The Upland was formed by the tension fault in Tertiary Period. The basement of the survey area is Parral Formation of early Cretaceous. The strike and the dip of the formation are NW-SE and 40° ~ 60° NE, respectively. The formation is mainly composed of compact and bedded shale layers which are partly intercalated with sandstone seams. The Pliocene andesite lava flows cover the formation with unconformity. Acidic rocks such as dacites and rhyolites intrude into the former two layers, and form low belt-type elongated hill area from south to north.

After Neogene, hard intrusive rocks are exposed by weathering and erosion, and form unique topography characterized by residual hills resulted from selective erosion caused by the differences of rock components. Throughout Quaternary, Parral River flows meanderingly forming terrace.

The history of mining in Parral area began in 1631, and the area is known as prominent mining district in Mexico. The veins in this district accompanied by intrusion of acid rocks yields large quantities of silver with zinc and lead. Gold with pyrite partly occurs in and near the contact area of the intrusive rocks.

4-2-2 Geology and geological structure

Geological interpretation of aerial photograph, field reconnaissance and drilling works are carried out in order to clarify the geology of Parral area. As the result of the survey, it was confirmed that the basement of this site is Parral Formation of early Cretaceous with the strike of NW-SE and the dip of 40° to 60° NE(Fig.4-2-1,4-2-2,4-2-3). The Parral Formation widely distributes in the southern part of the area,and is exposed along the southern side of Parral River including the tailing dam . Andesites of Oligocene cover the formation unconformably with the estimated strike of WNW-ESE and the dip of NNE. The

andesite distributes in the north-eastern part of the area and is exposed along the Parral River. Dacite and rhyolite of Oligocene distribute in the northern (north side of Parral River) and the eastern part of the area. They are exposed in the eastern part of the tailing dam across Parral River to form a series of hills of 150～300 m in width stretching from north to south. These acidic rocks are accompanied with rhyolite dykes of which direction is from south to north. They intrude into Parral Formation and andesite layer(Fig.4-2-1). There are terrace deposits along Parral River with over 5m in thickness. Clayey soil is mined in the northern side of the river,north of the Parral tailing dam,to manufacture bricks.

Fig.4-2-6 shows the fracture measurement site. Fig.4-2-7 shows Wullf's net of fracture directions. From this survey, The directions of N-S, NNW-WWE, and ENE-WNW are dominant. the existence of several faults is structurally presumed in the southern of the site to cut the Parral Formation and acidic rocks,with the direction of ENE-WSW. The nature of the faults is not well known, but judging from the topography,it is considered that the north-western side is comparatively subsided. Fig.4-2-4 shows the location of boring site. Fig.4-2-5 shows boring log.

(1) Cretaceous systems (Parral Formation)

Parral Formation was observed at B-3 drilling hole for the ground water observation. In D-1 and D-2 holes drilled for soil tests, only the observation of rock and stratigraphy was carried out using the cores. Detailed observation was carried out by using the core of B-3 hole. As the result of these observations, Parral Formation is mainly composed of shale partly accompanied with sandstone in the deeper part of GL.-6.75m at B-3 hole.

① Shale

The shale is the main member of the Parral Formation existing in GL. 6.75 to 39.65m at B-3 hole. The shale is pale greenish gray to gray white color and hard. The lamina has developed in it. Judging from the dip of the lamina, the dip of Parral Formation is estimated about 40° to 60° . The shape of drilling cores often have long columnar shape. The reason is not by lack of rock cracks but, quartz and pyrite veins developed in the fissures by mineralization adhere each

fragment. The pyritevein is sometimes accompanied with chalcopyrite. Most of the fissures are irregular. No shear joints was found.

② Sandstone

The sandstone exists in GL.39.65m to 40.00m at B-3 drilling hole. The rock is graysh white color, and arkosic and coarse-grained. The fissures are not observed in arkosic part.

(2) Tertiary (Oligocene) systems

The Tertiary System is composed of andesite, dacite and rhyolite including rhyolite dyke. The distribution of this System is in the northern and central part of this survey area.

① Andesite

The andesite exists in the deeper zone than GL.-3.10m in B-2 boring hole, and in the deeper than GL 8.90m in B-2 hole. The rock shows pale gray to grayish white color. The andesite is porphyritic with many feldspar and pyroxene phenocrysts. The rock is altered, but, hard and dense in B-1 and B-4 holes. The rock of B-2 hole is very ductive by alteration such as kaolinization or chlorinization. Pyrite is also crystallized in the rock.

② Dacite and rhyolite

These acidic rocks were not observed in boring cores, but, the outcropis found by the Parral mineral processing plant. The rocks show graysh white color, hard and acidic by silicification and kaolinization. They stretche from north to south along rhyolite dykes.

③ Rhyolite dyke

The dyke is a member of dacite and rhyolite above mentioned. A part of the dykes is exposed in the side of the Parral River. The rock is graysh white to pale yellowish white color and hard . It distributes stretching north to south intruding Parral Formation of Cretaceous period. Dykes are steeply exposed by differential erosion. The shape is easily recognized at a glance.

(3)Quarternary system

The Quarternary System is composed of terrace deposits and recent river deposits which distribute along the Parral River.

① Terrace deposits

The deposits are observed in the drilling holes of B-1, B-2 and B-3 for observation of groundwater. In the B-1 drilling hole located in the lowest reaches, the thickness of the formation is 3.10m and consists of gravel bed, silty fine-grained sand bed with gravels and mixture of sand and gravel bed from lower part to upper part.

In the B-2 drilling hole located at the center of the site,the thickness of the bed is 8.90 m and the bed consists of gravel bed, silty fine-grained sand with gravels, silty fine-grained sand bed, sandy silt bed and silty very fine-grained sand bed from lower part to upper part. In the B-3 drilling hole located in the uppermost reaches, the thickness of the bed is 6.75 m and the bed consists of very fine-grained sand, sandy silt bed, sandy silt bed with gravels, silt bed and fine-grained sand bed from lower part to upper part. The grading of sand and silt bed not including gravels is good, but, the grading is poor in the bed including gravels. These facts suggest that the environment of sedimentation was comparatively moderate near B-3 hole such as swamp. It is considered that the narrow,long bank of the acidic rocks of Tertiary from north to south might divide the environments of sedimentation of each side.

② Recent deposits

The deposits are on the river bed of the Parral River and mainly consists of rounded gravels of acidic rocks, andesites and shale. The gravels are poorly sorted .

4-3 Electrical Prospecting

4-3-1 Method of survey

The Schulumberger's Electrode Arrey was used in this survey which is the same method as in El Bote. Schinterx Model IPC7(2.5KW)was used and its maximum AB spacing of ANNB electrode system is 400m. The survey was carried out with 60 stations arranged on 21 lines. The location of the stations is shown in Fig.4-3-1.

Data of the survey were processed to analyse resistivity with the software for analysis (RESIX PLUS DC).

4-3-2 Result of survey

The analysed resistivity is classified into following four groups and is shown in Fig.4-3-2.

S Zone: tens to thousands of Ω · m

L Zone: Less than 100 Ω · m

M Zone: 100 ~ 200 Ω · m

H Zone: more than 200 Ω · m

L zone shows low resistivity, M zone shows medium resistivity, H zone shows high resistivity and S zone shows complex zone of low and high resistivity.

S zone forms the surface in thickness of 5m ~ 25m, the average thickness is 10m. Thick part of S zone is located around Parral dressing plant and the area along the Parral River. S zone is composed of the terrace deposits of recent and soil layer of weathered Cretaceous System and Tertiary System.

L zone forms the lower part of S zone around 1-12-28 line. Parral dressing plant and tailing dam are located along the line, and ground water is being pumped up from the underground of 400m of station 19. In the east and west side of the line, resistivity zone gradually changes to M zone or H zone. L zone is composed of shale of Cretaceous System. The L zone is formed in the lower part of S zone more than 150m thickness. L zone is composed of shale of Cretaceous.

M zone is formed around L zone and along the Parral River. M zone is composed of shale of Cretaceous System, andesite lavas and dacite intrusive rocks of Tertiary System.

H zone is formed in the area of shale and dacite intrusive area of Tertiary System in the eastern side of the dressing plant, and is formed in the area of andesite lavas of Tertiary System in the north-eastern part of Parral dressing plant.

The movement of groundwater was observed in a part of M zone, but was not observed in H zone. Therefore, it is presumed that M zone is aquitard, H zone is aquiclude or aquifuge.

L zone (low resistivity zone) distributes in the western area bordered andesite intrusives which lays north to the south, and M zone(medium resistivity zone) and H zone(high resistivity zone) distribute in the eastern area in geological structure. Parral River develops cutting the structure extending north to south, L zone is also formed along the river. It is considered that the L zone is controlled by main structure extending from south to north and crossing sub-structure.

4-4 Hydrology

The water system in the survey site is shown in Fig.4-1-1. Parral river gathers two branches which locate in the east and the west side of the tailing dam to the north, and flow down meandering from west to east. The purpose of this survey is studying the effect of tailing dam of CFM processing plant on the surface and groundwater. The survey of stream flow and water quality analysis were carried out at the points shown in Fig.4-4-1.

4-4-1 The surface water

Most of the rivers in the survey area except the main stream of Parral River dries up both in dry and rainy season. The flow rate of main stream of Parral River decreases in dry season, and the river is shallow enough cross on foot. However,in the rainy season, the flow rate of the main stream of the Parral River increases and the river changes to violent stream by the rapid increasing of precipitation in the upper stream area. According to the rising up of water level, the feature of flowing also remarkably changes. The waste water from the plant of private mine flows into the river near P-R1 point and the waste water from the underground mine is discharged into the Parral River at the northern bank of the river. In this survey, measurement of the flow rate of and water quality was carried out both in the dry and the rainy season at the following points.

In the dry season, measuring sites of stream flow are No.1 ~ No.5 and the sites of water quality are P-D1 and P-R1 ~ P-R5. In the rainy season,the sites of stream flow are No.1 ~ No.5 and the sites of water quality are P-D1, P-W1 and P-R1 ~ P-R5.

(1) The flow rate of surface water

The cross sections of the rivers were made at points No.1 ~ No.5 by this survey. At each point, the flow rate of (Cross-sectional area of flow) was calculated on the basis of current velocity data measured by Price flow meter using sectional plan of each point. The results are shown in Table 4-4-1 and Fig.4-4-2.

Considering the Fig.4-4-2 shown above, the flow rate gradually decreases from upper to lower reaches in dry season. On the contrary, the flow rate increases from upper to lower reaches in rainy season. The fact means that the flow rate is affected by seasonal factor such as precipitation and evaporation. There is remarkable difference in three sections between the point No.1 ~ No.2, between No.2+No.3 ~ No.4 and between No.4 and No.5.The reason is presumed as follows;

① Variation of rate in the dry season

i) Increasing in the flow rate between the points No.1 ~ No.2.

There are CFM plants on the western bank and private mine on the eastern bank in this section. The muddy waste water from the latter plant is heavily discharged, and almost all the waste water at No.2 can be considered to come from this private mine.

ii) Decreasing in flow rate between the points No.2+No.3 ~ No.4

The flow rate of stream flow of 2,060.7m^3/day is the total amount at No.2 and No.3. The amount of the rate of stream flow decreases to 1,453.2m^3/ day at No.4. The large amount of water of 607.5m^3/day disappears in this section. The distance of this section is only about 250m to 300m. The evaporation and seepage is considered not to affect the disappearance. There is no divergence of water in this section. It is most possibly estimated because there are large amount of deposits consisting of sand and gravels along the wide range of riverbed in the section between No.3 ~ No.4, therefore, almost all the water decreased in this section makes under flow of the river deposits. Therefore, the apparent rate of streamflow decreases in this section.

iii) Decreasing in flow rate between the points No.4 and No.5

The distance of this section is 2.39km, the river flows down among the villages meandering with big curvature. Andesite is exposed on the riverbed and the bank, the thickness of the river deposits may not be so thick. The reason of the disappearance of 500m^3/day of water is considered to be caused by water consumption, pumping up from shallow well and evaporation.

② Variation in flow rate in rainy season

i) Increase in the flow rate between No.1 ~ No.2

The river bed around No.1 point was dried up just like in dry season. The waste water from private mine is considered to represent almost all the surface water of the branch at No.2.

ii) Increase in flow rate between No.2+No.3 ~ No.4

The feature of the main stream of Parral River in the rainy season is different from that in the dry season. The river becomes turbid current with movement of large amount of soil and sand. The flowing route of stream changes rapidly and the width of the river increases. As there are much river deposits in this section, the difference of the flow rate shows approximately 7,000m^3/day between the two points and this is considered to penetrate to become underflow at No.3, and flow up to the surface water near No.4.

iii) Increase of flow rate between No.4 ~ No.5

There are wide exposed rocks in this section and deposits on the riverbed may not be thicker than in the upper stream. Therefore, it is considered that not only underflow water is added to surface water but also much water from the branches is added.

③ Viriation and nature of flow rate in the dry and the rainy season

The main stream of Parral River dries up in the dry season. On the other hand, it changes to turbid current in the rainy season. Seasonal differences of the flow rate is remarkable in the main stream of Parral River as above mentioned. The order of the flow rate in the dry season is 103m^3/day. On the other hand, in the rainy season, it increases to 106m^3/day. However,the flow rate near the tailing dam has no seasonal change. The reason is considered that precipitation

amount of rainy season and dry season remarkably varies in the upper stream area of Parral River in spite of small amount of precipitation in this area.

(2) Water quality of surface water

The sampling of surface water was carried out at the 9 points of P-D1,P-W1 and P-R1 ~ P-R7 in order to analyse pH and contents of pollutants (Table 4-4-3). The rate of streamflow of Parral River in the dry season and the rainy season remarkably fluctuates, and muddiness of water also changes.

① P-R3 Point

Point P-R3 is located in the upper reaches of CMF plant. The water in this area is comparatibly clear which does not include pollutants except Fe in the dry season. The surface water flowing in the river is transparent. The surface water changes to muddy and it includes almost all the pollutants except Cr^{+6} and CN in the rainy season. Particularly,Pb, Fe and Hg contents exceed the upper limit of the Environmental Standard of Pollutants Content(Table 4 -4-2) in the rainy season. The rising of the flow rate in Parral River is due to increasing of precipitation in the area of the upper reaches. Considering the phenomena, pollutants within the surface water are diluted and the contents of pollutants decrease. But, there are some mines in the northern bank of just the upper reaches and some big branch flown into Parral River there, because waste water, slime and polluted materials deposited on the riverbed is presumed to be agitated by rain and flow into the Parral River in the rainy season.

② P-R4 Point

P-R4 point locates in the junction of Parral River and the southern branch into which the waste water from CMF plant and private plant are discharged. Various pollutants are detected having no connection with the season. It means that the pollutants are continuously supplied from the southern branch. By the data of the rainy season, the aspect is not obvious due to the supply of the same pollutants from the upper reaches of Parral River. By the data in the dry season, pollutants such as Cu, Pb, Zn, Fe, Cd, Total Cr, Cr^{+6} and CN are obviously supplied from this branch (Fig4-4-3). Particularly, CN does not naturally exist but is used in the plant. Consequently, the pollution up to

P-R4 point is obviously affected by the waste water from CMF plant. In the rainy season CN is not detected due to dilution by the increased river water.

③ P-R5 ~ P-R7 Point

The components of the sample in P-R5 ~ P-R7 points are similar. They contain no Cr^{+6} and CN, and have the same ratio of component, But, in the sample in P-R7, total Cr slightly increases and exceeds the upper limit of the Environmental Standard. It is considered to be affected by the branch flowing from the north. The amounts of pollutants has not big difference with comparison of the analysed data both in the dry season and in the rainy season. Seasonal change is not considered to affect the water quality.

④ P-W1 and P-D1 Point

P-W1 is from the CMF plant. All the waste water of the plant is discharged to the tailing dam. The chemical components of the waste water and the surface water at P-D1 show almost the same nature as show in Table 4-4-3. For mine water pumped up from P-M3 point is used as milling water in this plant, the surface water is obviously affected by the mine water. The chemical components of the samples of P-W1 and P-D1 were affected mostly by chemical components of milling ore and amounts of reagents for milling(particularly CN). It is slightly affected by seasonal change at P-D1 point.

Cr^{+6} is not detected and CN is always detected at P-W1 and P-D1 points. Cu, Pb and Total Cr exceed the upper limit of the Environmental Standard in the data of the dry season. Zn, Fe, Cd and Hg is added to the former components in the data of the rainy season. As mentioned before, CN was detected at P-R4 point along the main stream of Parral River in dry season. It is confirmed the pollutants flown out from the slime of the plant contaminate Parral River. Judging from Fig. 4-4-3, the data of Cu, Pb, Zn, Cd and Total Cr gives backup of this idea. It is not obvious in the rainy season, however, Pb and Fe also contaminate this area.

⑤ P-R1 and P-R2 Point

P-R1 point is at the junction of a branch and route of waste water from the private plant that locates on the opposite side of the branch in the eastern

part of the tailing dam. The sample of this point has slightly different nature from the surface water of CFM dressing plant. As shown in Fig.4-4-3, the contents of Fe and As in the dry season, and Pb, Fe and As contents in the rainy season exceed the upper limit of the Environmental Standard. The pollution of the water reach up to P-R2 point both in the dry and rainy season. It is obvious that the private dressing plant is the major origin of the pollution of Fe and As. However, the influence of the pollution of As on the main stream of Parral River has not detected yet.

Cr^{+6} was detected only at two points of P-R1 and P-R2 only in the dry season. There is no obvious origin of Cr^{+6} in this area, however, the points are located in the distribution area of intrusive rocks. Cr^{+6} is possible to be supplied from the mineralization zone that is accompanied with the intrusive rocks.

Pb and Fe contents at P-R5 point in lower reaches exceed the upper limit of the Environmental Standard in the dry season and As was also detected. The waste water is discharged from the southern side of the river. Pollution of the area is considered to be caused by the waste water.

At P-D1,pH was 8.90 which shows strongest alkalinity in the dry season in this area. Except this sample, pH of the other samples are 8.20～8.84 which means weak alkalinity. They are not affected by the tailing dam.

PH of the sample at P-D1 shows strong alkalinity of 11.05 in the rainy season. The influence spreads to the points P-R1 and P-R2 along the southern branch where pH is over 9.00. But, the influence is not detected in the main stream of the Parral River. pH of the samples of P-R3 ～P-R7 along Parral River are 7.80 ～ 7.97 which constantly shows weak alkalinity (Fig.4-4-3).

The pollution of this area shows areal characteristics due to increasing of the rate of streamflow. on the other hand, local characteristics in this area becomes vague in the rainy season. On the contrary, local characteristics is enhanced in the dry season. As the result, origin of pollution and the pollutants were defined in this area.

4-4-2 Ground water

Electric prospecting and the survey of the rate of streamflow(current speed) with boring holes and analysis of water quality were carried out in order to examine the influence of the waste water from CFM mineral processing plant and

the tailing dam on the groundwater.

(1) The flow rate of groundwater

4 observation holes, 3 of the holes of B-1 ~ B-3 locate along the Parral River from the lower reaches to the upper reaches, and B-4 hole near the curving point were drilled. The survey of the aquiferous layer level and the measurement of current speed of groundwater were carried out. The results are shown in Fig.4-2-5 of Columnar Section By Boring, Table 4-4-4 and Fig.4-4-4 of Current Speed of Groundwater. The aquiferous layer observed in drilling holes are shown in Fig.4-4-4, 4-4-5, and 4-4-6.

① Aquiferous layer

i) B-1 hole Aquiferous layer within Neo-Tertiary andesite
approximately EL 1,727 ~ 1,731 m

ii) B-2 hole Aquiferous layer within Neo-Tertiary andesite
approximately EL 1,732 ~ 1,735 m

iii) B-3 hole Aquiferous layer within Terrace deposits
approximately EL 1,742 ~ 1,745 m
Aquiferous layer within slate of Parral Formation of Cretaceous
approximately EL 1,712 ~ 1,742 m

iv) B-4 hole Aquiferous layer within Neo-Tertiary andesite
approximately EL 1,744 ~ 1,745 m

The equiresistivity plan was made in the depth of EL.1,710 m, EL. 1,720m and EL.1,730 m as Fig.4-4-5 in order to examine the distribution of aquiferous layer. As the result, in EL.1,710 m and EL.1,730 m low resistivity zone is cut by the area of intrusive rocks and the zone only continues in EL.1,720 m.

The mapping of shallower part than EL.1,740 m which mostly consists of Quarternary deposit is difficult because of big variation of data.

By the reason mentioned above, the distribution of aquiferous layer can be considered in the same layer of low resistivity zone of 150 Ω · m. The current direction is not obvious. However, judging from the topography, groundwater is considered to flow to NE direction roughly.

The review is summarized in Table 4-4-5.

② Seasonal change of groundwater

The seasonal change of the groundwater reflects in the change of average current speed. The groundwater level markedly differs in the dry season and in the rainy season. The groundwater level in the rainy season rose approximately 0.2 m from that of the dry season in B-1 hole. There is no water in B-2 hole in the dry season, but, the groundwater existed in approximately 5.3～5.8m from the bottom in the rainy season. In B-3 hole, the difference of the groundwater table became more marked, and the water table reaches at approximately 19.3～19.6 m from the bottom in the rainy season.

Therefore,as the marked falling of the groundwater table is considered to occur in the dry season around the CMF plant in the survey area, the flow rate naturally decreases and the effect is estimated to appear in the area where the ground water flows down as shown in Fig.4-4-5. The major reason of the decrease in the flow is due to pumping up the large amount of mine water at P-M1～P-M3. To eliminate the effect of pumping up, it is necessary to keep the groundwater level around B-3 hole over EL.1,730m (GL.-19.15m), and if the average current velocity assume 0.0103m/sec as shown Table 4-4-4, increments of 0.637x106m^3/day is at least necessary to anticipate.

(2) Water quality of groundwater

Groundwater is sampled at P-B1～P-B4 and P-M1～P-M3 in order to analyse the contents of ten kinds of heavy metals including measurement of pH. Table 4-4-6 shows the results of chemical analysis.

① P-B1(B-1 hole) Point

The contents of pollutants at P-B1(B-1 hole) are generally higher than the contents of surface water at P-R5 in spite of neighboring P-R5. Pb and Fe contents in the dry season exceed the upper limit of the Environmental Pollutants Content. Addition to the Pb and Fe contents,Hg content in the rainy season also exceeds the upper limit of the Environmental Standard. The waste water flows into from the south in this point, the waste water is considered to penetrate and concentrate pollutants. Marked high content of Fe is a characteristics.

② P-B2(B-1 hole) Point

P-B2(B-1 hole)is neighboring P-R6. The components of the surface water at P-R6 and the groundwater at P-B1(B-1 hole) are resemble, and Pb and Fe contents of both the water exceed the upper limit of the Environmental Standard.

③ P-B3(B-3 hole) Point

In the groundwater at P-B3(B-3 hole), Pb and Fe content exceed the upper limit of the Environmental Pollutants Content in the dry season. The groundwater table markedly differ in this point, by approximately 11.5 m between in the dry season and the rainy season. Therefore, the difference of the level is considered to have some relationship with the change of the nature of groundwater. Comparing with the component of the groundwater at P-M3 which locates in the south-west of P-B3, Zn and Cd contents are markedly higher than that of the other samples. There is same nature that Pb, Zn, Fe and Cd contents exceed the upper limit of the Environmental Pollutants Content. It means the groundwater of the same nature, which pumping up near P-M3 exists in shallow part at P-B3. The groundwater at P-M3 is pumped up from GL.-150m (EL.1,614m) and GL.-135m(EL.1,629m).

④ P-B4 Point

The nature of the groundwater at P-B4 is generally the same of the water at P-B1 ~ P-B3, and the contents of Pb and Fe only exceed the upper limit of the Environmental Standard.

⑤ P-M1 and P-M2 Points

P-M1 and P-M2 locate in the western side of Parral River. The chemical components and their contents are resemble closely. It is considered that the samples are collected in the same layer. The distribution of this layer correspond with the distribution of acidic volcanic rocks which accompany rhyolite dykes. The layer and the acidic volcanic rocks are considered to have some relationship. The groundwater at P-M1 is pumped up from GL.-82m(EL.1,672m), and the groundwater at P-M2 is pumped up from GL.-65m (EL.1,696m), respectively. Judging from the pumping up level, the groundwater is considered to be within the acidic volcanic rocks in the depth described above.

⑥ P-M3 Point

The groundwater at P-M3 pumped up from GL.-135m(EL.1,614m). The contents of Pb, Zn, Fe, Cd and Hg exceed the upper limit of the Environmental Standard. The groundwater generally includes much heavy metals. It means that the water exists in mineralized zone. This affects the groundwater at P-B3 as already mentioned. Because the groundwater is used as the milling water, the surface water in the tailing dam is also affected.

About pH, as shown Fig.4-4-3, pH becomes lowest around P-M3 and is acidity, however, in the lower reaches of the distribution area of rhyolite dykes, all pH are within 7.28 ~ 7.69 except the sample at P-B4 (B-4 hole) to show weak alkalinity.

⑦ Penetrating Water from the tailing dam

Considering the effect of penetrating water from the tailing dam on the groundwater, the surface water at P-D1 is pumped up from P-M3, in this stage the water is acidity(pH is around 4), and is discharged after using as milling water. The water quality becomes acidity to strong alkalinity during milling, chemical component of the water is affected by the groundwater at P-M3. On the contrary, Cu and Total Cr which exceeds the upper limit at P-D1 are less in all other samples, and CN was not detected at all. Therefore, penetrating water from the tailing dam hardly affects the groundwater in present condition.

4-4-3 Groundwater Flow System Simulation

Optimum simulation blocks of physical and hydraulic properties are modelled around the Parral Mine. A Groundwater flow system is simulated under the condition of these properties which are obtained by integrating the results of meteorological, geological, hydrologial surveys and soil test.

By this simulation, clarified are water table, flow direction and flow speed. Simulation results are contributed to calculate effective goundwater harness, waste water recycle and mining pollutant dispersion.

(1) Simulation Method

A numerical simulation for groundwater flow is conducted by the use of three dimension simulator "GWS3D2P" originally developed by Dr. Hiroyuki Tosaka of

Tokyo University. In this simulator, Darcy's law and mass balance equations are analysed by Finite Difference Method. The details of this simulator is described in Appendix A "Numerical Simulation Technology for Subsurface Fluid Flow".

(2) Simulation Model

① Block Model

Simulation area takes the form of rectangular, 3.0km wide in the north-south direction and 2.0km wide in the east-west direction (Fig.4-4-8). The Parral mine is located in the southern side of the area. From this mine tunnel the groundwater is pumped up for mine plants, slime and the sewerage system of Parral municipality. This pumping brings drawdown of grounwater level.

The veins and fissures mainly strike north-south and subordinately strike east-west around the Parral ore deposits. These veins and fissures control groundwater flow direction. The simulation area is framed to predict the drawdown and waste water dispersion. Consequently, the direction of the simulation area is in accordance with the vein strike. and the area is decided to cover the mine and the pump site. The simulation depth is decided to 1,500m above sea level, because of the pumping 150m below the surface at the municipality water supply site (P-M3 site in Fig.4-4-9) in the mine tunnel.

The simulation area is divided into 30 blocks in the north-south direction, 20 blocks in the east-west direction. The block size is evenly 100m × 100m wide . X and Y axes of this area are in the directions of east-west and north-south, respectively. The coordinates of the south-west end and north-east end are (X1,Y1), (X20,Y30), respectively.

Vertically, the area is divided into 9 underground layers and 1 atmoshere layer, total 10 layers. The uppermost atmosphere layer is the first layer named Z1. Surface layers are 10 to 20m thick, deep site layers are 50m thick. The height of each block is represented by the elevation of the center of the block.

② Permeability and Porosity Model

Permeability and porosity of each simulation block are determined by integrating the geological,geophysical and hydraulic properties.

Geologically, the southern part of the simulation area is underlain by Cretaceous mudstones. The northern part is underlain by Tertiary andesite

lavas and its pyroclastic rocks. The parral river is running across the boundary of both parts. Dacite intrudes these Cretaceous and Tertiary rocks in the north-south direction. These rocks are usually compact and not permeable except around the veins and fissures along the Parral river.

As the results of the electrical prospecting and boring observation, low resistivity zone and low-high complex resistivity zone correspond to aquifer. Intermediate resistivity zone corresponds to aquitard. High resistivity zone corresponds to aquiclude and aquifuge.

As compared with geology and geological structure, The aquifer zone is equivalent to vein, boundary of the intrusive rock, sandy terrace deposit ,and fault zone. The aquitard is equivalent to weathered overburden and fault periphery. The aquiclude is equivalent to surface soil and calyey terrace deposit. The aquifuge is equivalent to the compact Cretaceous, Tertiary or intrusive rocks.

As the results (Table 4-4-7) of grain size distribution, the aquiclude permeability coefficient of clayey terrace deposit ranges 10^{-5} to 10^{-7}cm/sec (BR-1 to BR-7). 10^{-5}cm/sec is dominant. Consequently, the aquiclude permeability coefficient is set to 10^{-5}cm/sec.

Around the Parral mine, several veins and faults are developed in the Cretaceous and Tertiary rocks. Permeability coefficient of these fractures is different from its peripheral rocks. this permeability coefficient of these fractures is named fracture permeability coefficient (pkf). To the contrary, the permeability coefficient of the peripheral rocks is named matrix permeability coefficient (pkm). From this basis, The average permeability coefficient (K) of the simulation block is calculated as follows.

$$K=(hef/\triangle X) \times pkf+(1-hef/\triangle X) \times pkm$$

$\triangle X$:width of fracture

hef:width of block

The porosity is also distinguished fracture porosity (porf) from matrix porosity (porm) and is given the value corresponds to the hydraulic observation.

Table 4-4-8 shows the permeability coefficient and porosity model, and Fig.4-4-9 shows the rock classification maps on the basis of this concept. At the Parral mine, several big veins are embedded. The veins have been mined 1 km long along the strikes, 200m wide and 200m deep below the surface. So, the

permeability coefficient of the vein zone is presumed to be 10^{-3}cm/sec, because the vein zone corresponds to big fault zone.

Fig.4-4-9 shows rock classification. In this plane map (X-Y CROSS SECTIONAL VIEW), the coordinates of left-bottom and right-top ends are (X1,Y1) and (X20,Y30), respectively. In the cross section (Y-Z CROSS SECTIONAL VIEW), left and right ends are Y30 and Y1, respectively. The legend No. of Table 4-4-8 corresponds to it of Fig.4-4-9.

③ Hydraulic Model

The Parral river flow down from west to east near the Parral mine. As Fig.4-4-1 shows, No.4 river flow measuring point is situated upstream of the Parral river. At this No.4 point, flow rate is 1,453m^3/day in the dry season and $1.967 \times 10^5 m^3$/day in the rainy season. The flow rate is various ,because its large drainage basin area collect large quantities of the river water. Therefore, The flow rate $1.967 \times 10^5 m^3$/day is set in the rainy season during June to October, 1,453m^3/day in the dry season during November to May at No.4 point for simulation.

The tributary stream running eastern side of the Parral mine has no riverwater through the year. At this stream the initial flow rate is not set for simulation.

Each Water level of the observation wells is set for simulation as to be situated at the top of the third layer counted from atmosphere layer. However, at the several undergrounds of the Parral mine, groundwater is pumped up as Fig.4-4-8 shows. Therefore, the water level of the P-M1 and P-M2 pumping sites are set at the top of the sixth layer, which water levels are 82m and 65m below the surface, respectively The P-M3 site's is set at the top of the seventh layers, which water level is 150m below the surface.

As the result of chemical analysis of groundwater, P-M3 water shows strongly acid of pH 4.8 and high chemical components in contrast with the riverwater, P-M1 and P-M2 sites groundwater which show weakly alkaline. From this fact, the P-M4 water, near the P-M3 site, is inferred to be deep seated origin similar to mineral spring and to flow upwards through the vein at the rate of 2,000m^3/day, 200m below the surface, 1,550m above sea level. The P-M4 site is set at the top of the ninth layers,

④ Meteorological Model

Annual precipitation is 500mm on the average during 1977 to 1990. 95 percent of it precipitate during rainy season from June to October. Therefore, during these 5 months, the precipitation is 475mm from June to October. During other 7 months the precipitation is 25mm.

Evaporation data are referred from New El Coco observation. Evaporation of it ranges 0.35 to 0.84mm/day.

Recharge rate is set as 0mm/day during dry season, 2mm/day during rainy season, by precipitaion minus evaporation.

⑤ Recharge Discharge Model

Groundwater of the Parral mine is pumped up at three sites. P-M1 site is at the rate of 450m^3/day, from the sixth simulation layer, and 82m below the surface. P-M2 site is 450m^3/day, the sixth layer, and 65m below the surface. P-M3 site is 7,800m^3/day, the seventh layer, and 150m below the surface. The mineral dressing plant of the Parall mine discharges waste water at the rate of 400 m^3/day from P-W1 site, which is the second simulation layer.

(3)Simulation Results

Fig.4-4-10 shows groundwater saturation map. Rainy season map is of the 150th day, counted from the first day of rainy season. Dry season map is the 360th day, counted from the first day of rainy season. In this maps, blue color is 100% saturated with free water. in accordance with the changing blue to brown, the saturation level decreases.

The Parral mine area (Site A on the map) shows higher saturation degrees of the surface layers of the second and the third layers in the rainy season, compared with the dry season. it means the higher water level in the rainy season than dry season in the Parral mine area. But,in the dry season, pumping the groundwater from the mine causes drawdown of the water level. The influence extends to the opposite northern side over the Parral river and eastern side of the mine. This influence decreases in the rainy season.

On the other hand, the downward area along the Parral river (site B)shows the same saturation level during both the dry and rainy seasons as shown in the third layer.